

Effect of the substituents on the $^1\text{O}_2$ production and biological activity of $(\text{N}^{\wedge}\text{N}^{\wedge}\text{N})\text{Pt}(\text{py})$ complexes.

Guillermo Romo-Islas,^{a,b} María Gil-Moles,^{c,d} Arnav Saxena,^a Antonio Frontera,^e
M. Concepción Gimeno^{c,*} and Laura Rodríguez^{a,b,*}

^a *Departament de Química Inorgànica i Orgànica, Secció de Química Inorgànica, Universitat de Barcelona, Martí i Franquès 1-11, 08028 Barcelona, Spain. e-mail: laurarodriguezr@ub.edu*

^b *Institut de Nanociència i Nanotecnologia (IN2UB). Universitat de Barcelona, 08028 Barcelona, Spain*

^c *Instituto de Síntesis Química y Catálisis Homogénea (ISQCH), CSIC-Universidad de Zaragoza, Pedro Cerbuna 12, 50009 Zaragoza, Spain. e-mail: gimeno@unizar.es*

^d *Departamento de Química, Centro de Investigación de Síntesis Química (CISQ), Universidad de la Rioja. Complejo Científico-Tecnológico, 26004, Logroño (Spain)*

^e *Departament de Química, Universitat de les Illes Balears, 07122 Palma de Mallorca,*

Supporting Information

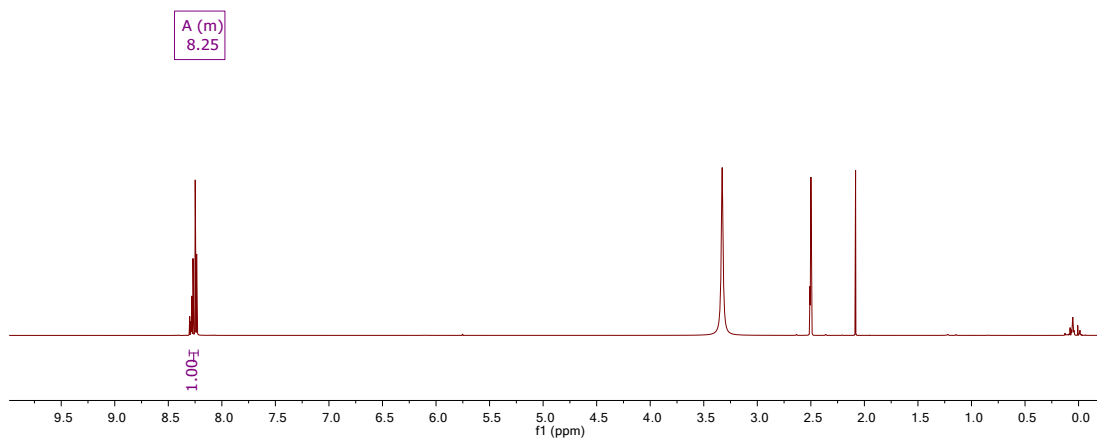


Figure S1. ^1H NMR spectrum of ligand H_2L^3 in $\text{DMSO}-d^6$.

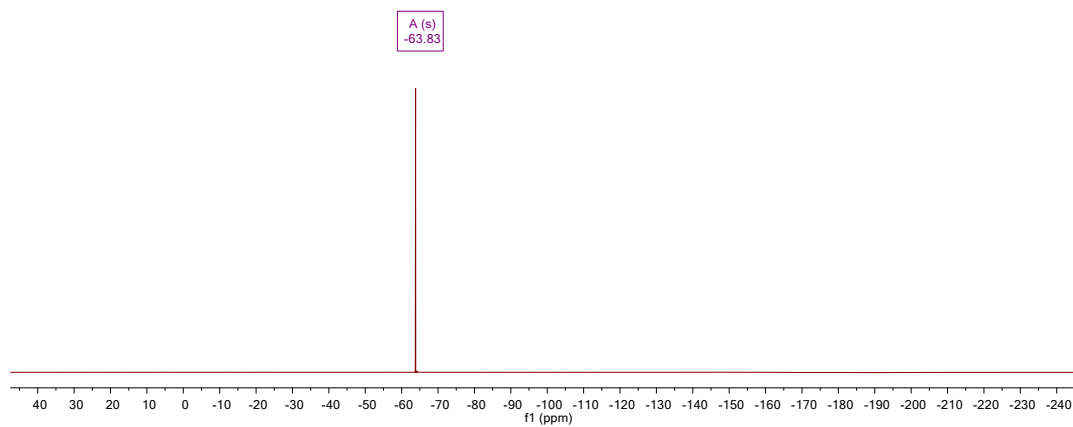


Figure S2. ^{19}F NMR spectrum of complex H_2L^3 in $\text{DMSO}-d^6$.

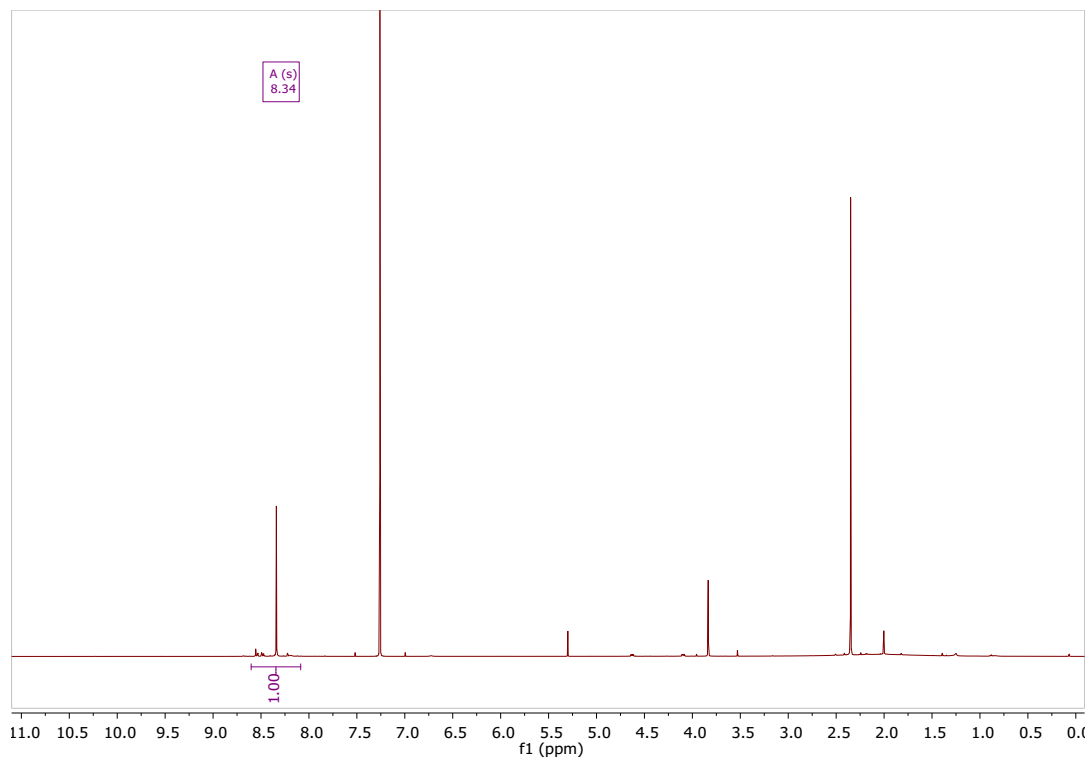


Figure S3. ^1H NMR spectrum of ligand H_2L^4 in CDCl_3 .

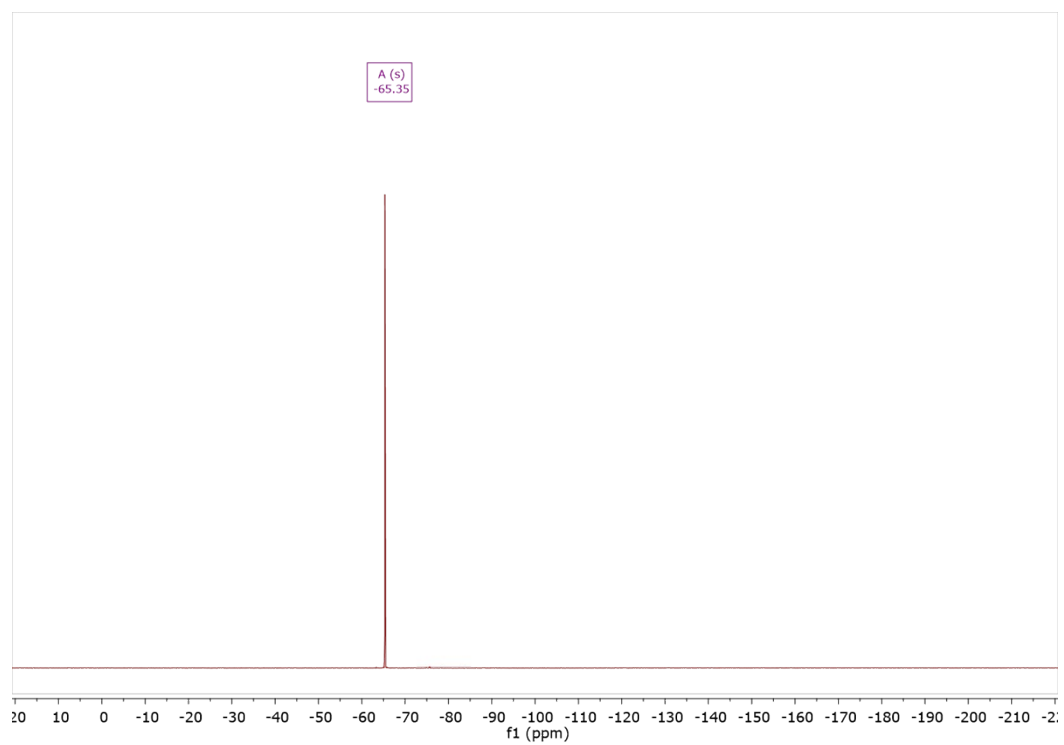


Figure S4. ^{19}F NMR spectrum of complex H_2L^4 in CDCl_3 .

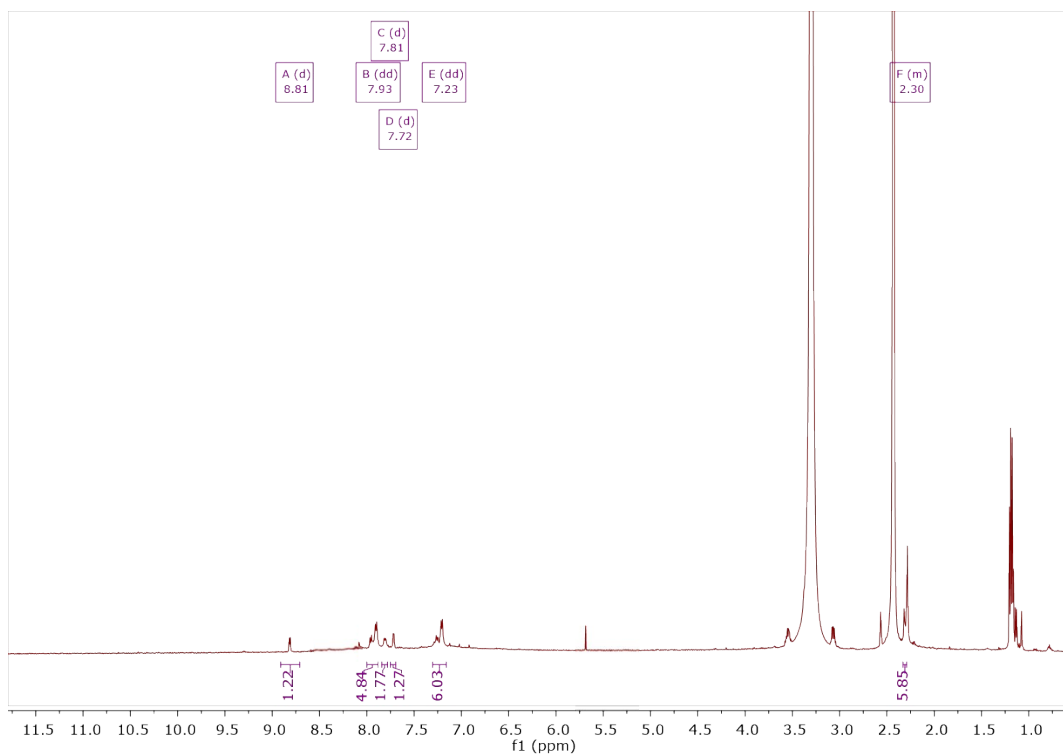


Figure S5. ¹H NMR spectrum of complex 1-CF₃ in DMSO-d₆.

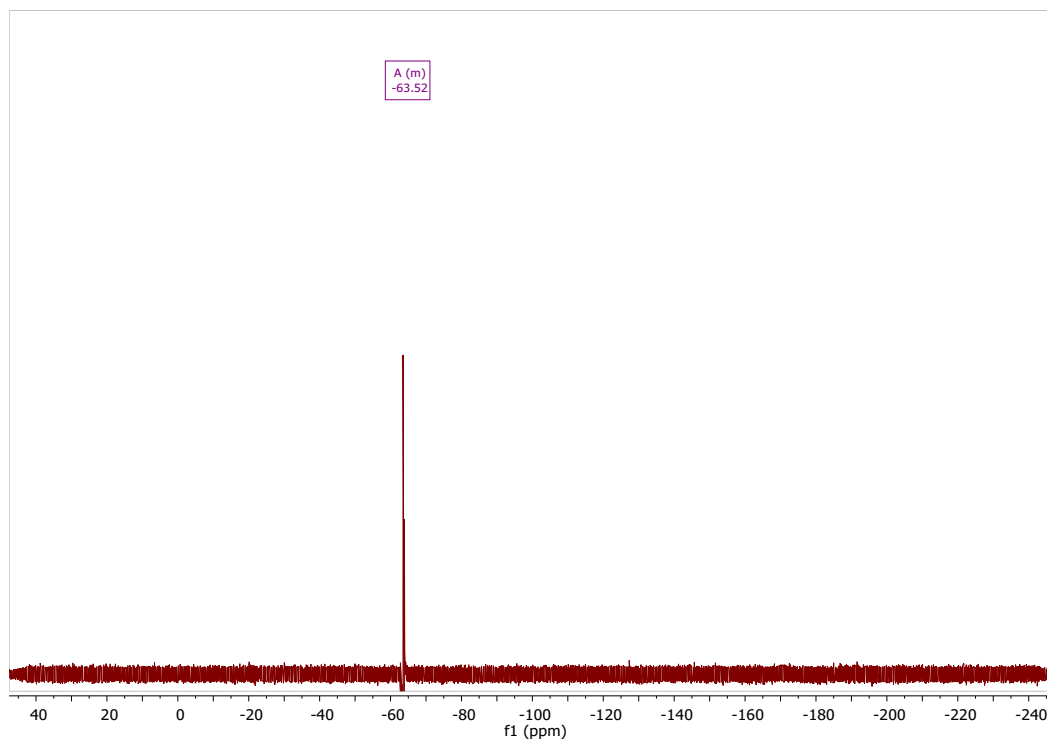


Figure S6. ¹⁹F NMR spectrum of complex 1-CF₃ in DMSO-d₆.

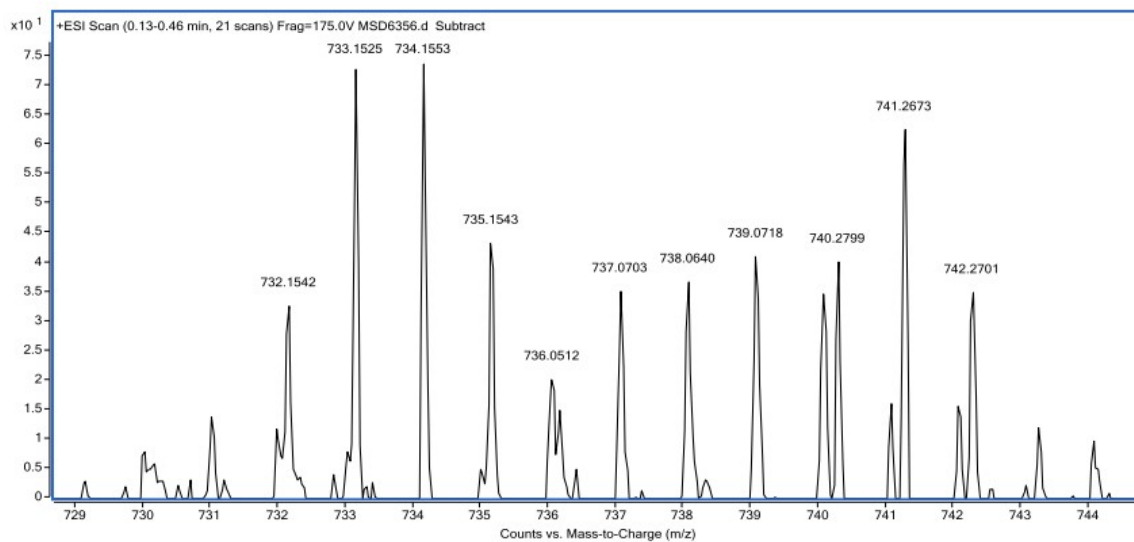


Figure S7. ESI-TOF(+) of complex **1-CF₃**.

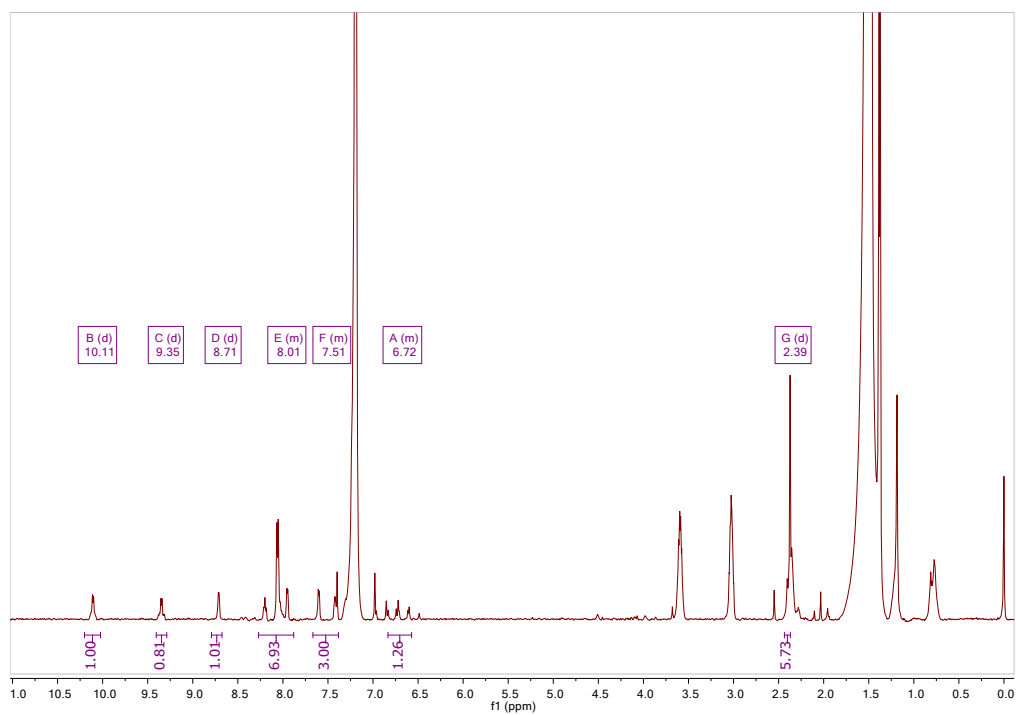


Figure S8. ¹H NMR spectrum of complex **1-CHF₂** in CDCl₃.

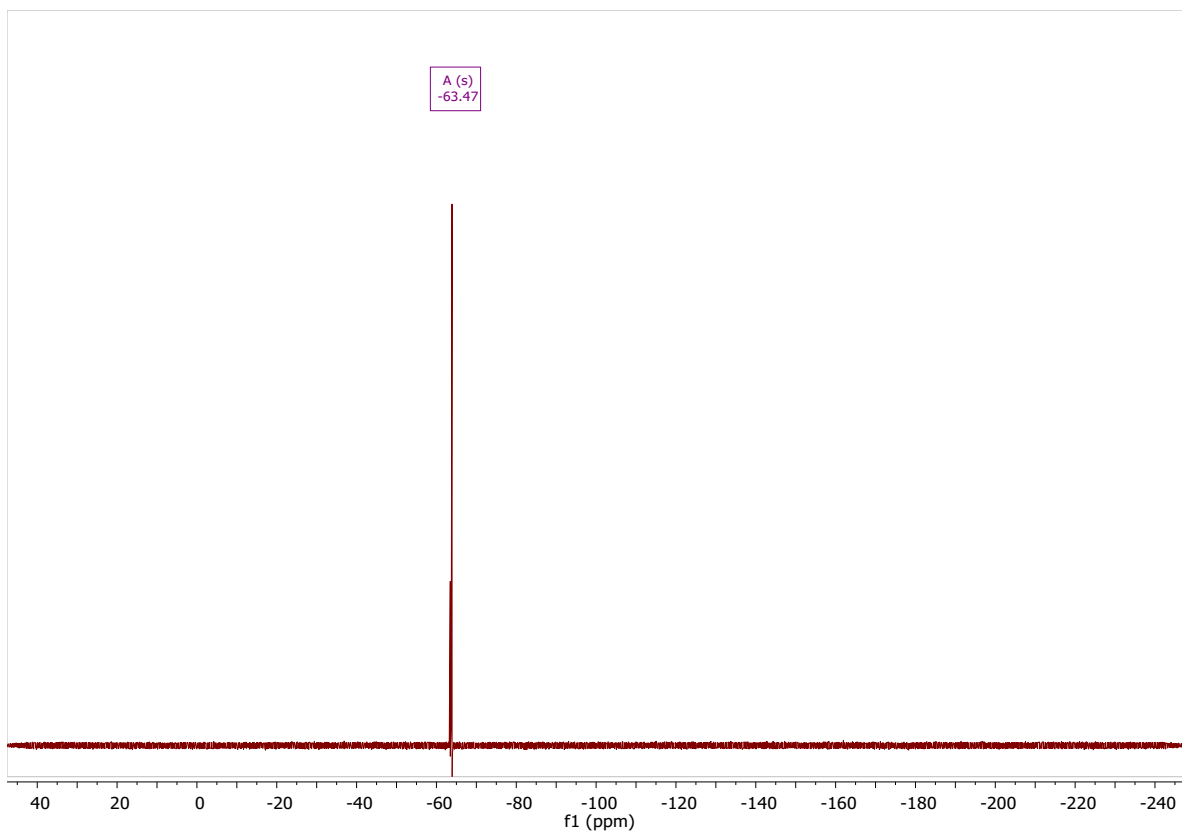


Figure S9. ^{19}F NMR spectrum of complex **1-CHF₂** in CDCl_3 .

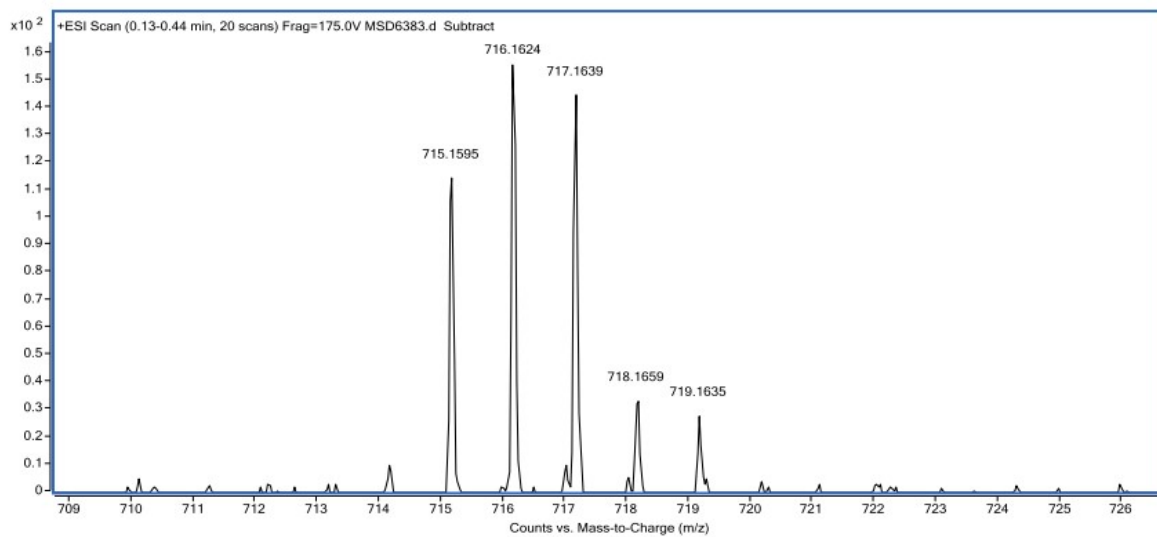


Figure S10. ESI-TOF(+) of complex **1-CHF₂**.

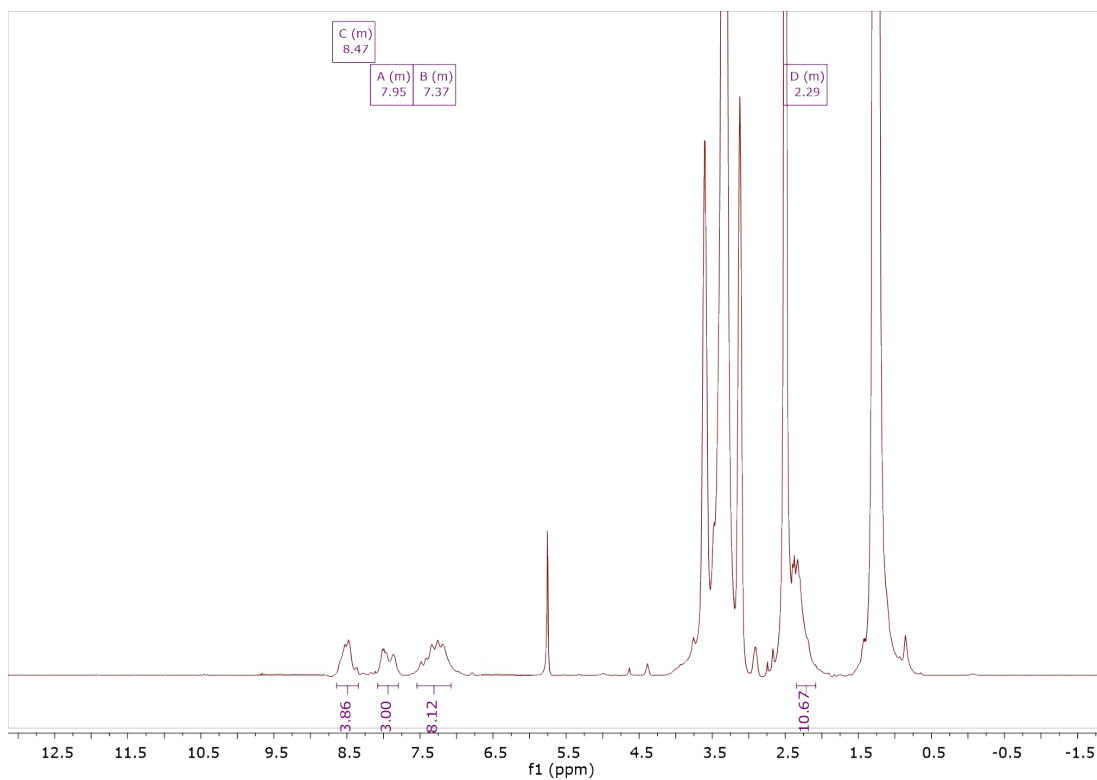


Figure S11. ^1H NMR spectrum of complex **1-CH₃** in $\text{DMSO-}d^6$.

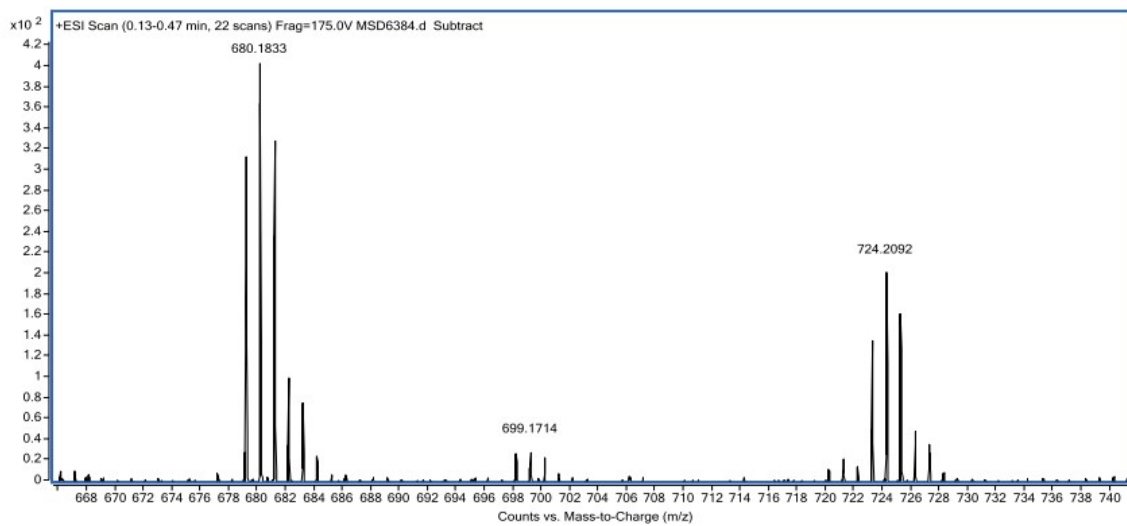


Figure S12. ESI-TOF(+) of complex **1-CH₃**.

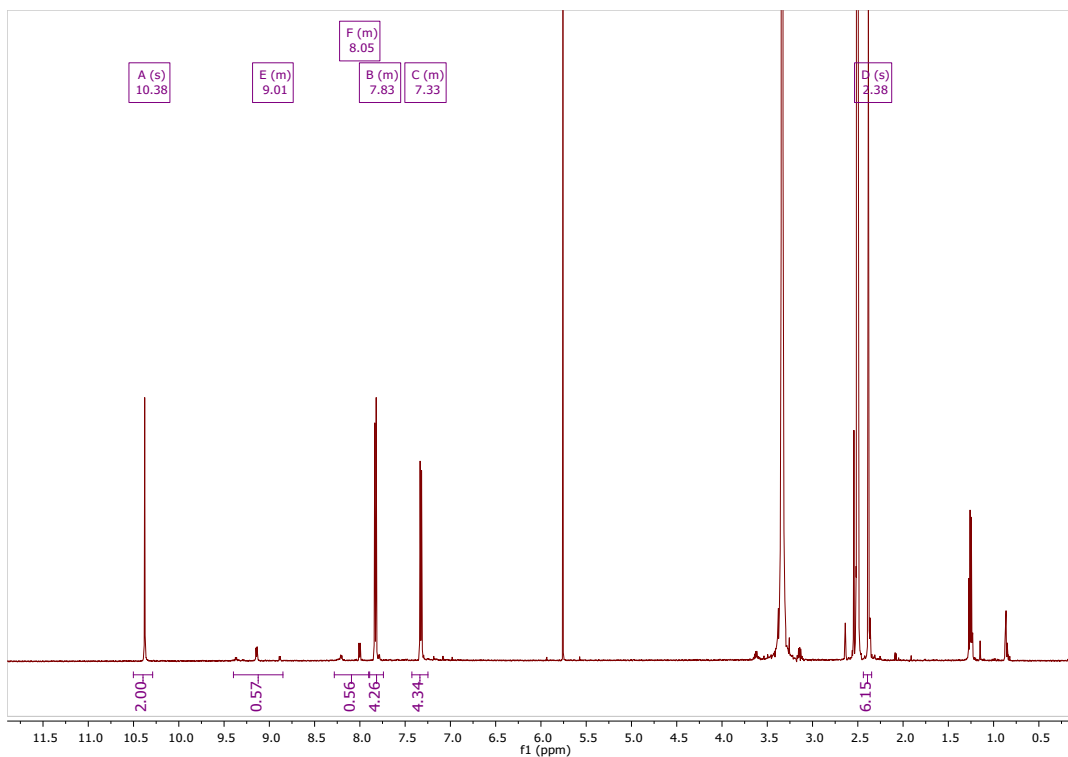


Figure S13. ^1H NMR spectrum of complex 2-CF_3 in $\text{DMSO-}d^6$.

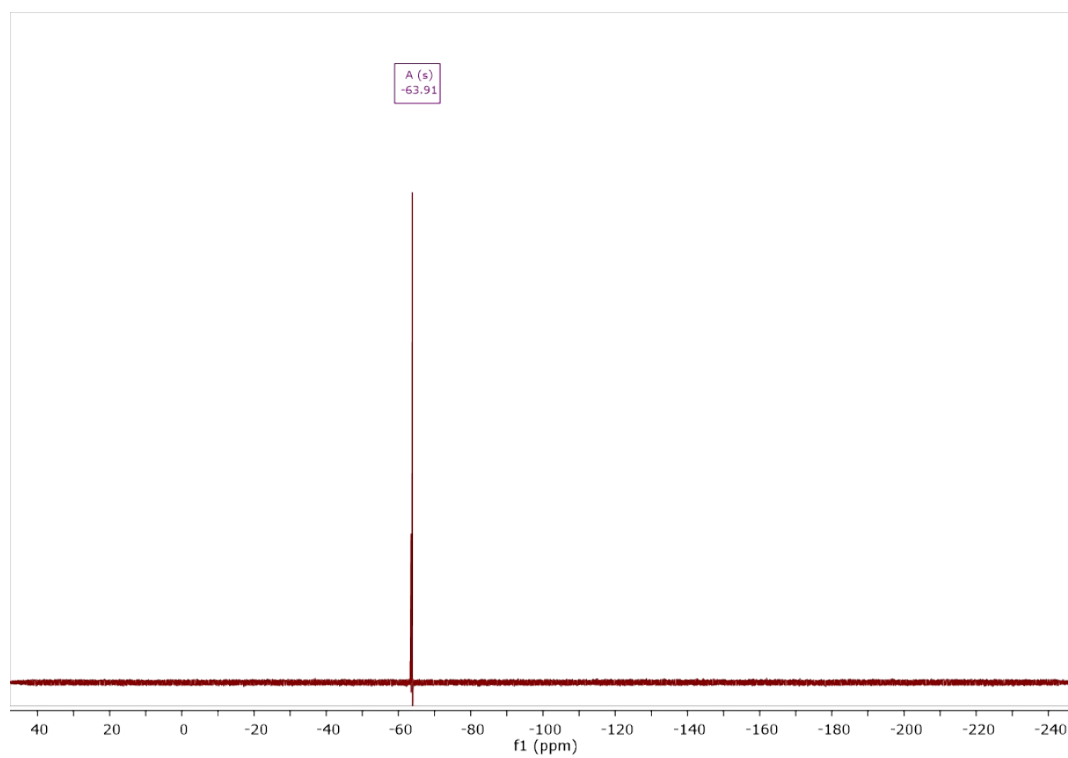


Figure S14. ^{19}F NMR spectrum of complex 2-CF_3 in $\text{DMSO-}d^6$.

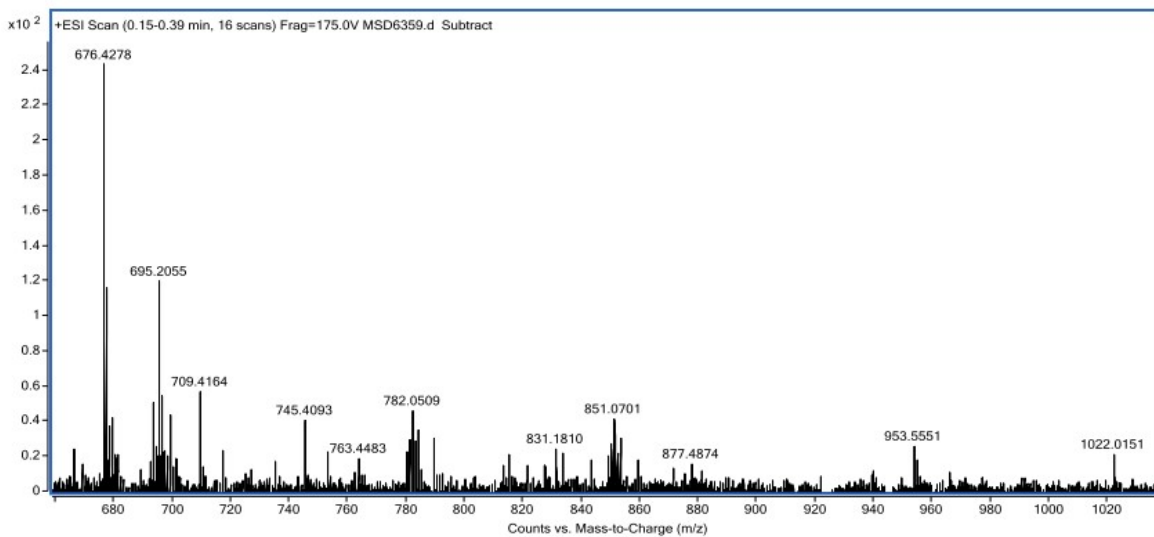


Figure S15. ESI-TOF(+) of complex **2-CF₃**.

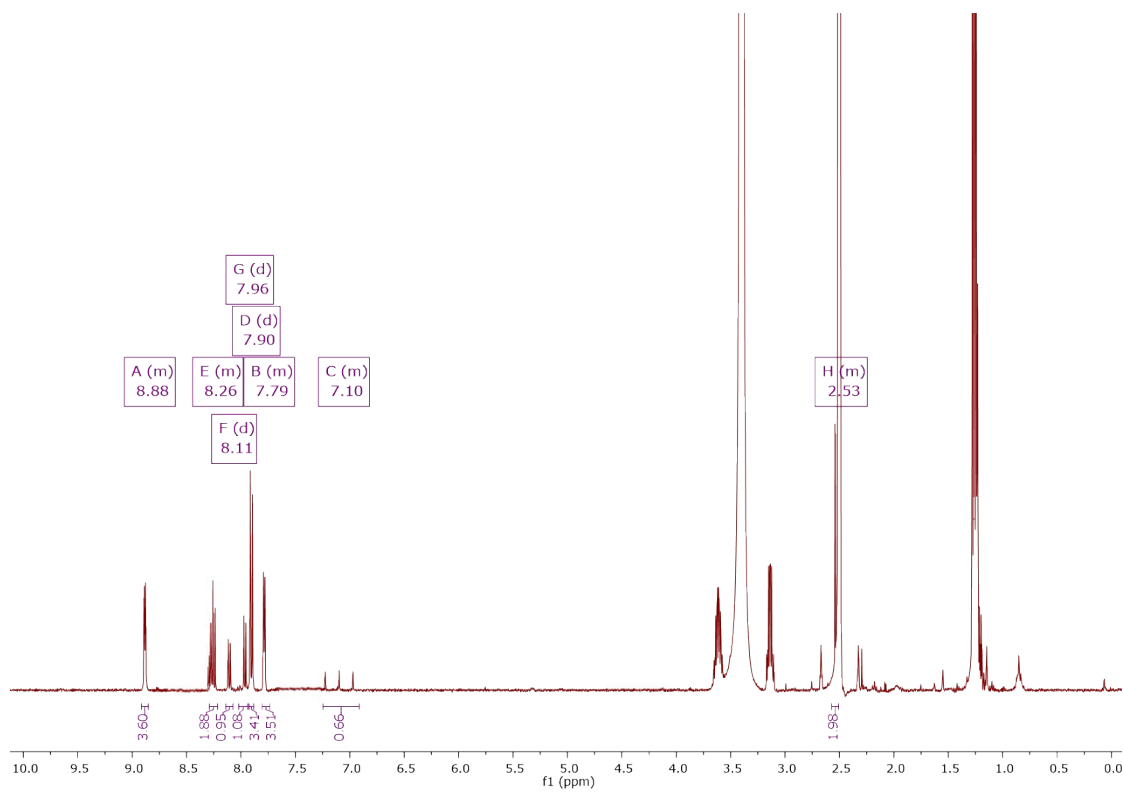


Figure S16. ¹H NMR spectrum of complex **2-CHF₂** in DMSO-*d*⁶.

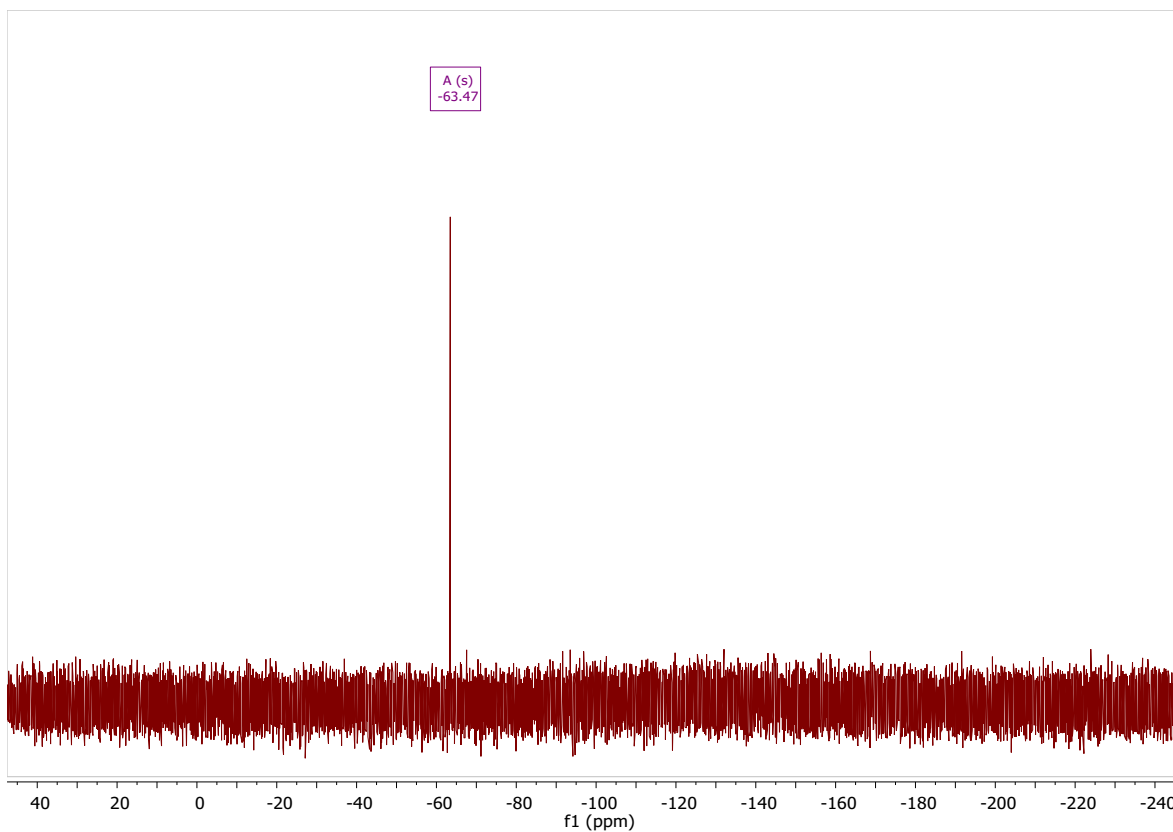


Figure S17. ^{19}F NMR spectrum of complex 2-CHF_2 in $\text{DMSO-}d_6$.

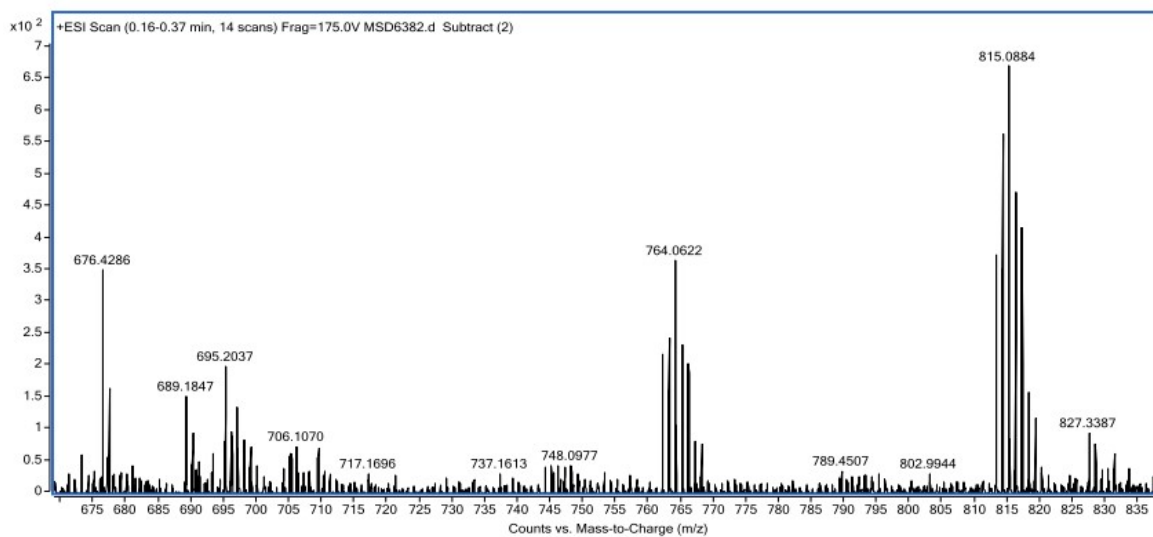


Figure S18. ESI-TOF(+) of complex 2-CHF_2 .

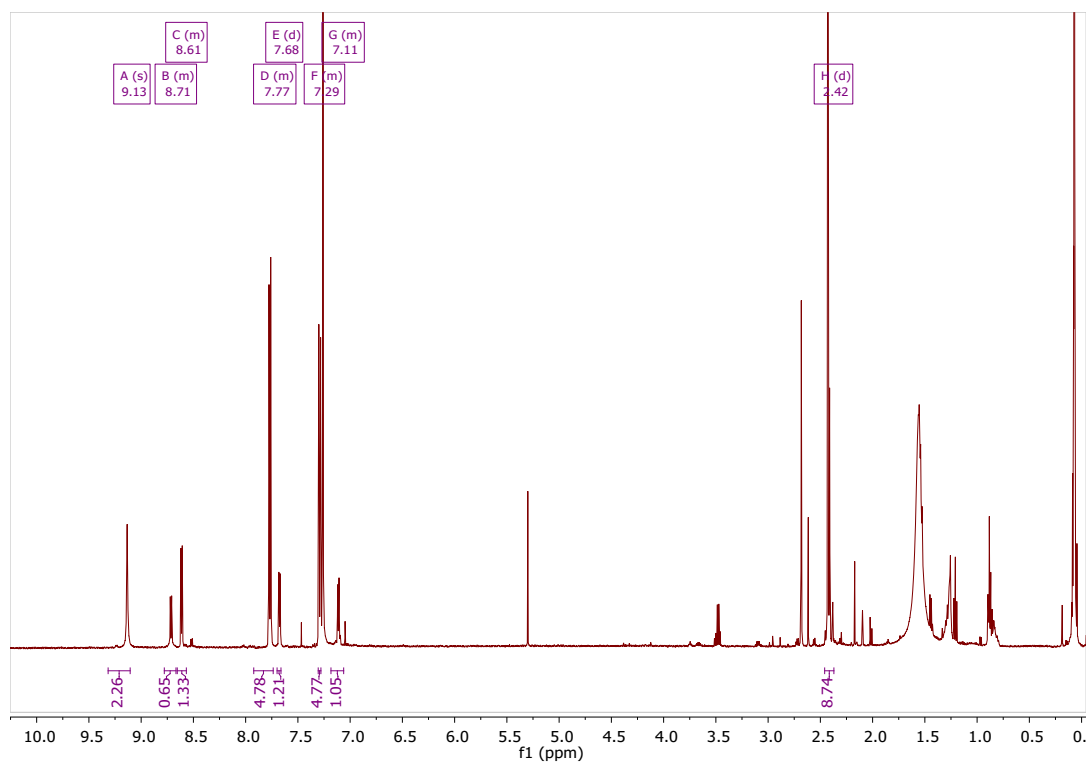


Figure S19. ^1H NMR spectrum of complex **2-CH₃** in CDCl_3 .

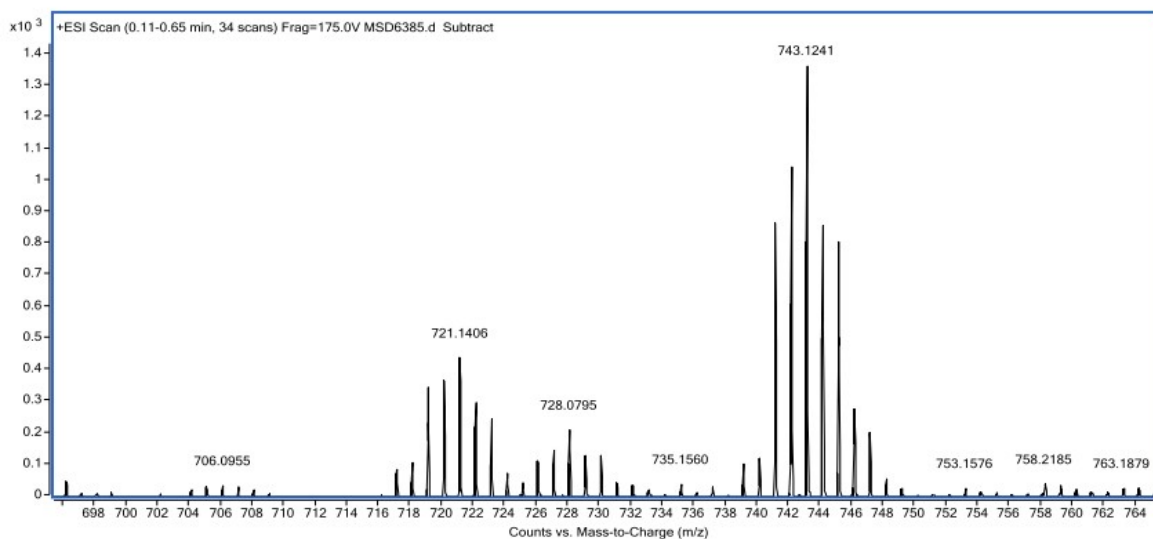


Figure S20. ESI-TOF(+) of complex **2-CH₃**.

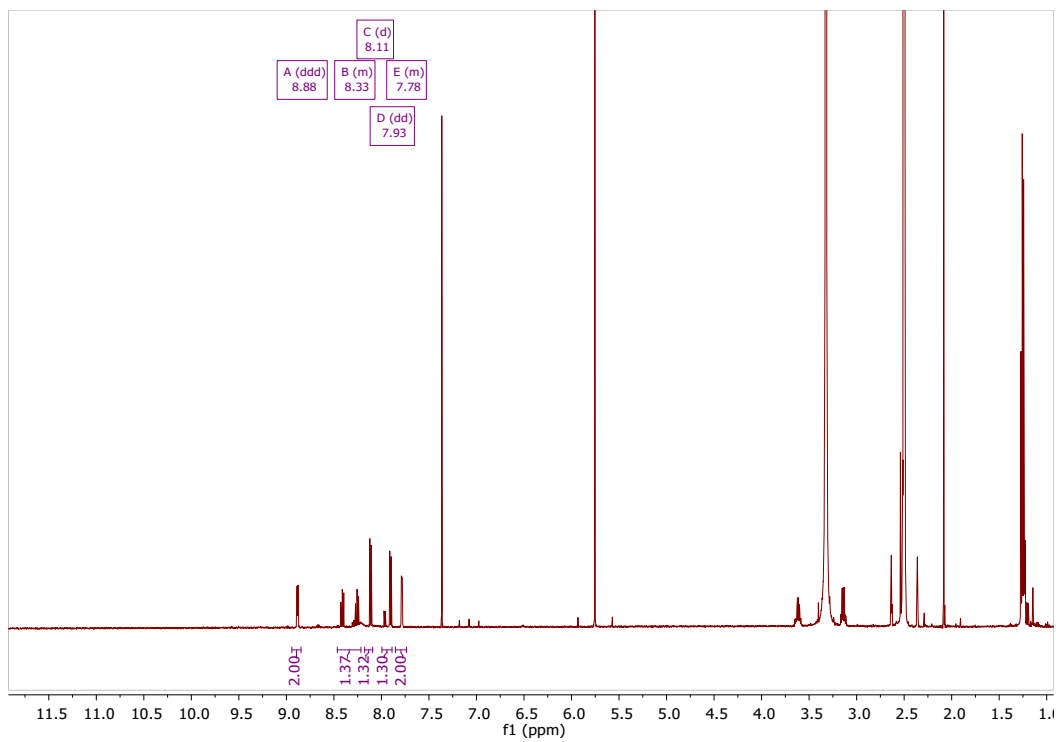


Figure S21. ¹H NMR spectrum of complex 3-CF₃ in DMSO-*d*⁶.

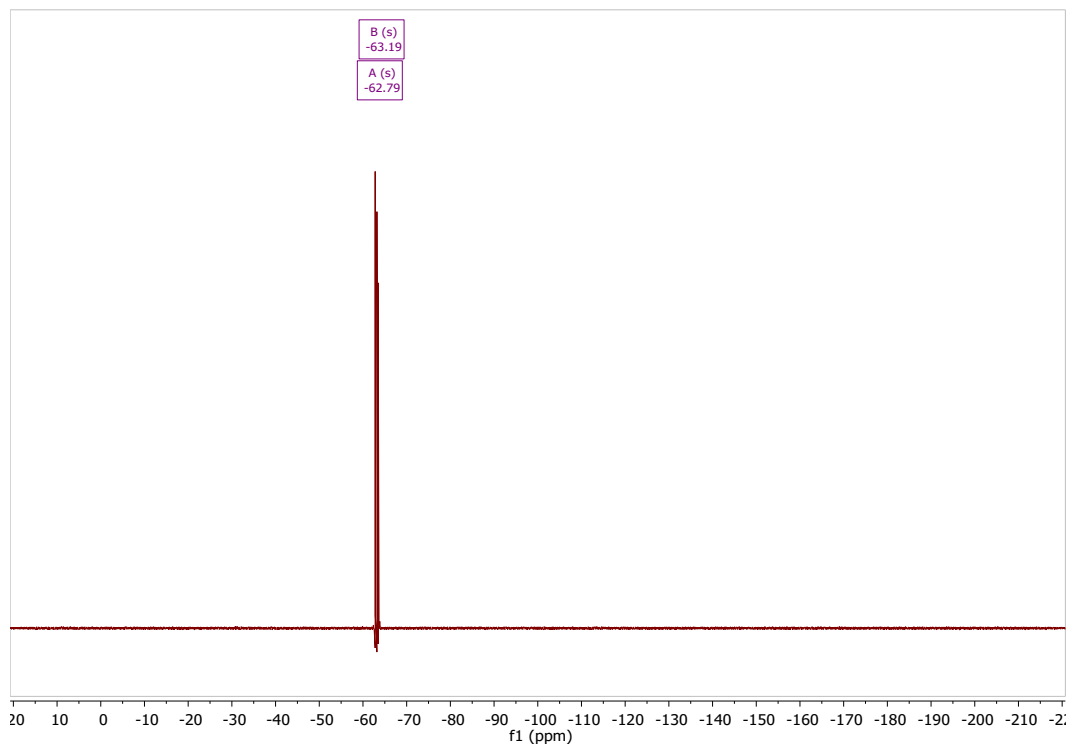


Figure S22. ¹⁹F NMR spectrum of complex 3-CF₃ in DMSO-*d*⁶.

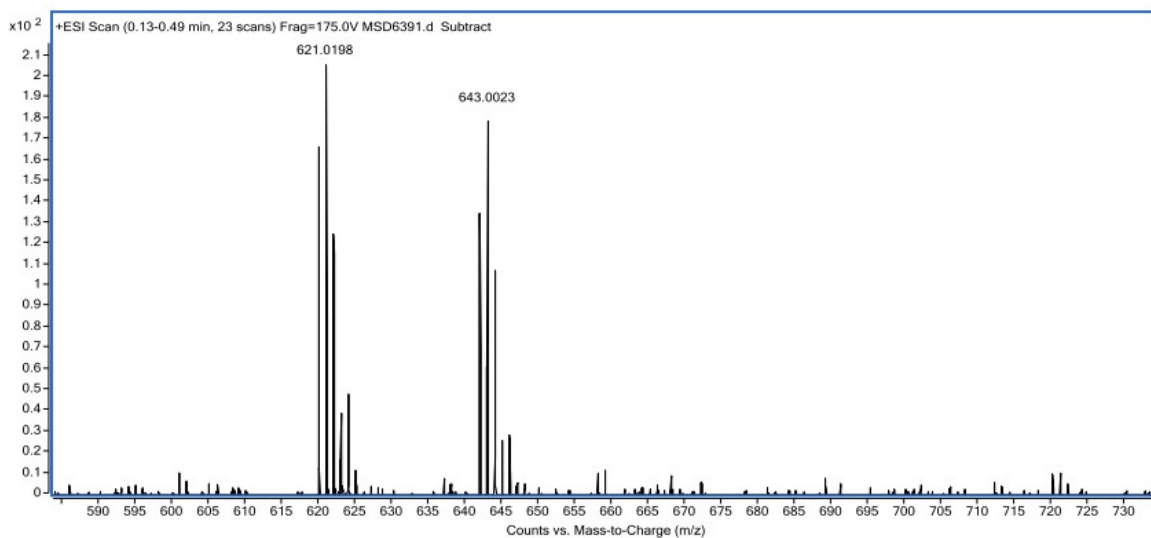


Figure S23. ESI-TOF(+) of complex **3-CF₃**.

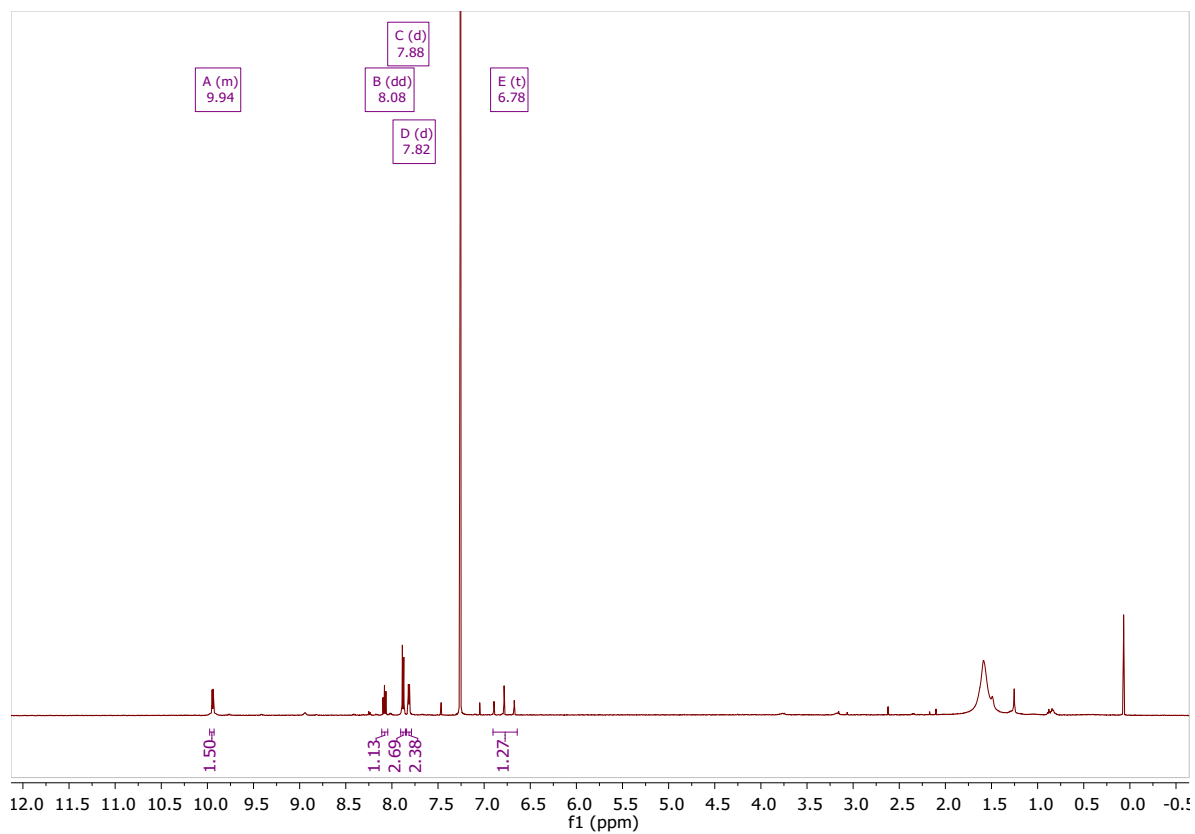


Figure S24. ¹H NMR spectrum of complex **3-CHF₂** in CDCl₃.

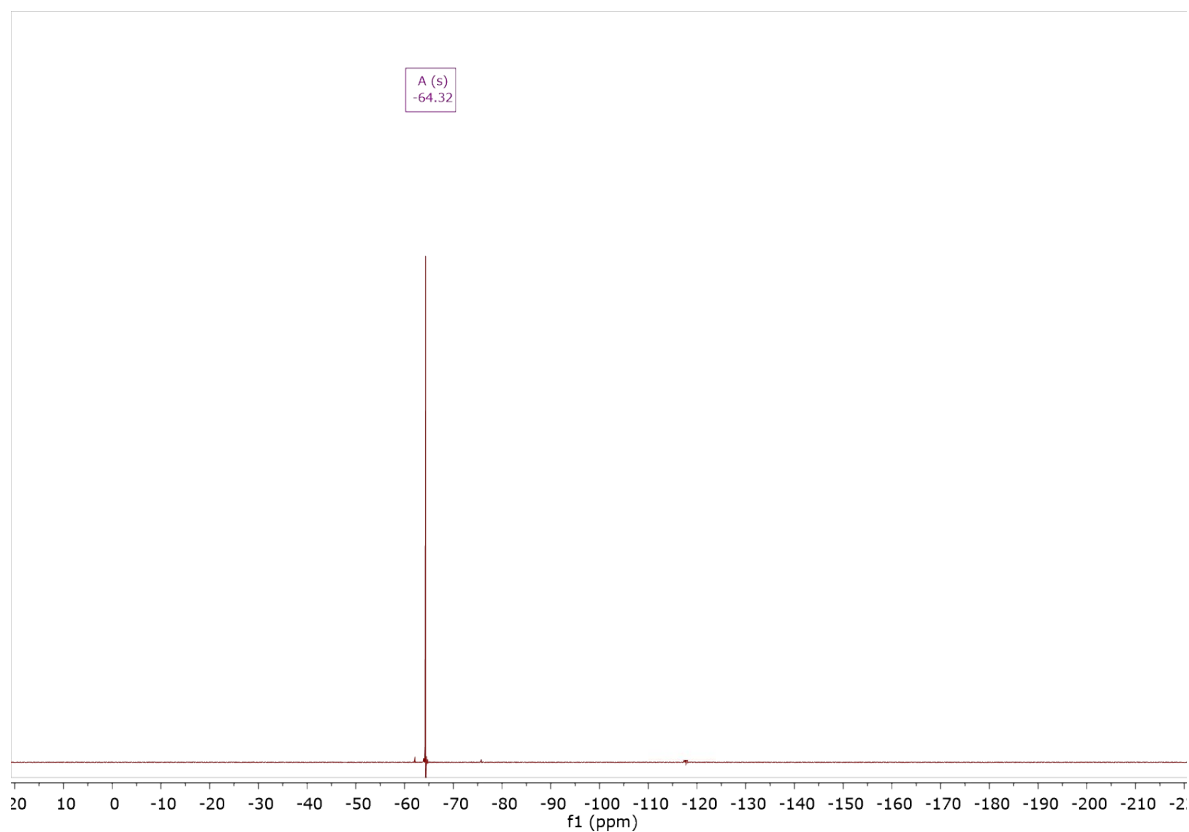


Figure S25. ^{19}F NMR spectrum of complex **3-CHF₂** in CDCl_3 .

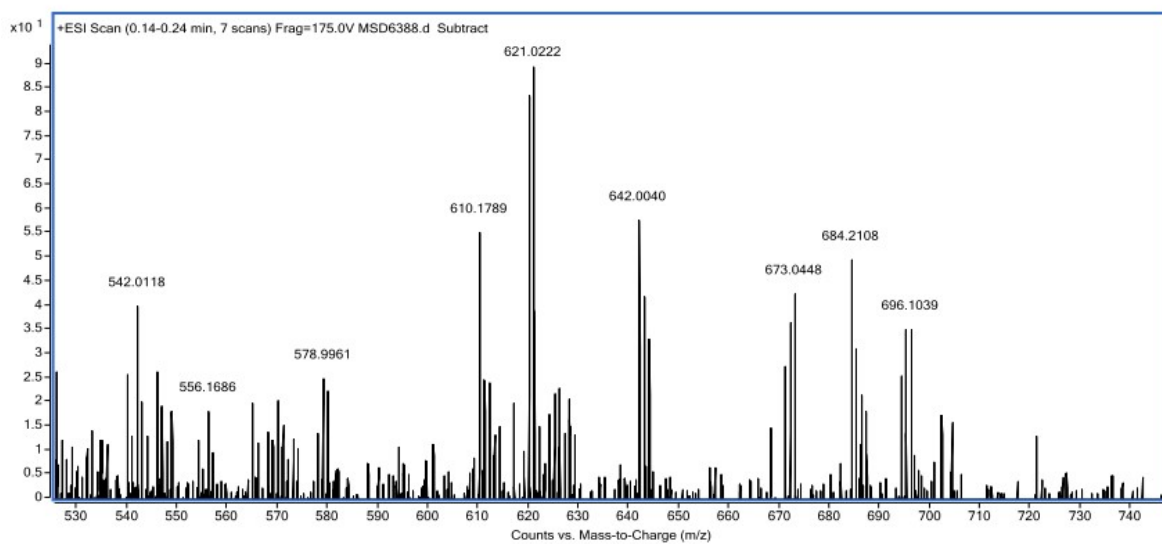


Figure S26. ESI-TOF(+) of complex **3-CHF₂**.

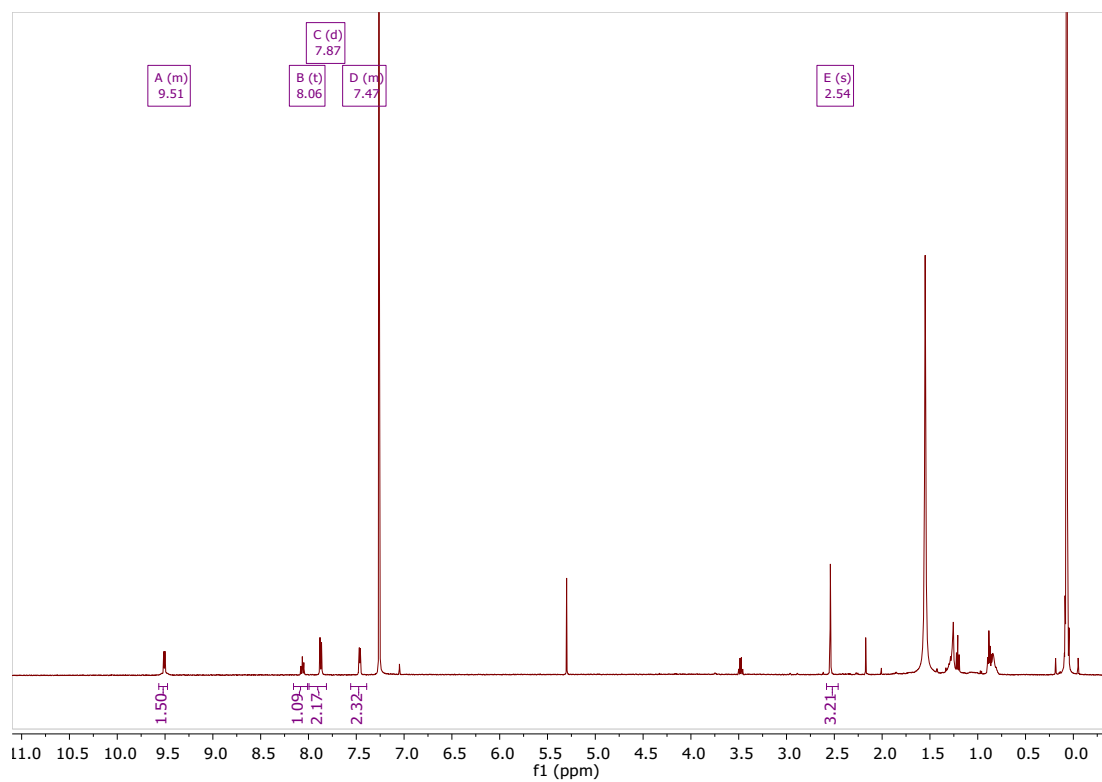


Figure S27. ^1H NMR spectrum of complex **3-CH₃** in CDCl_3 .

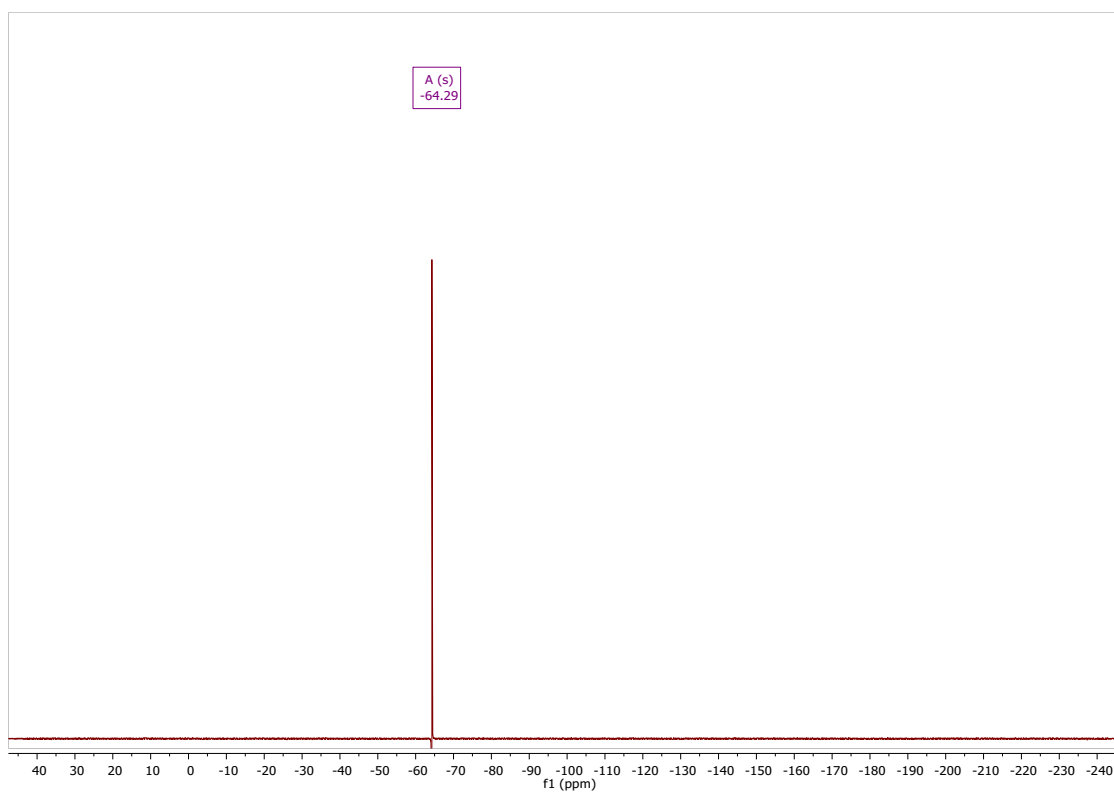


Figure S28. ^{19}F NMR spectrum of complex **3-CH₃** in CDCl_3 .

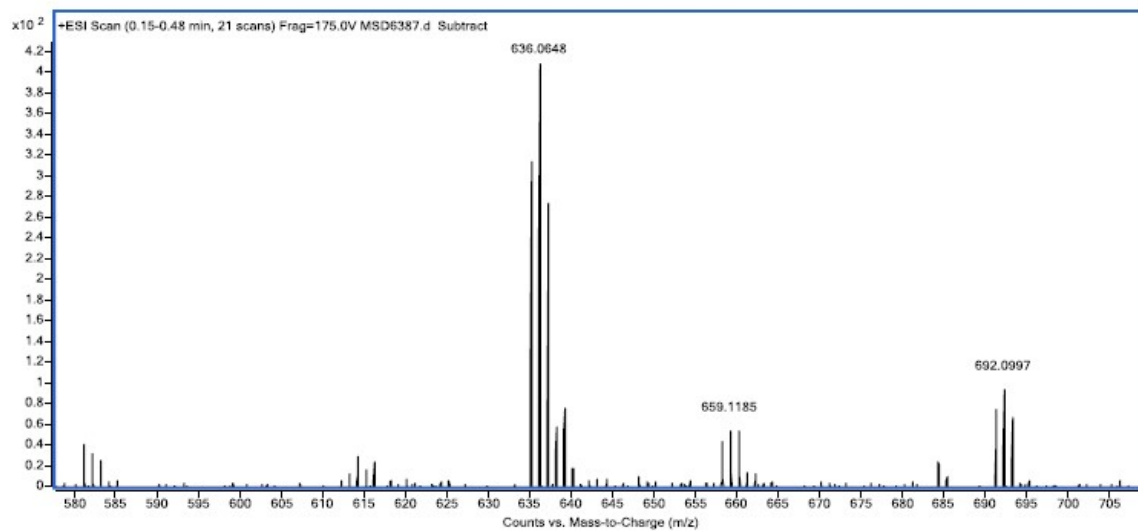


Figure S29. ESI-TOF(+) of complex **3-CH₃**.

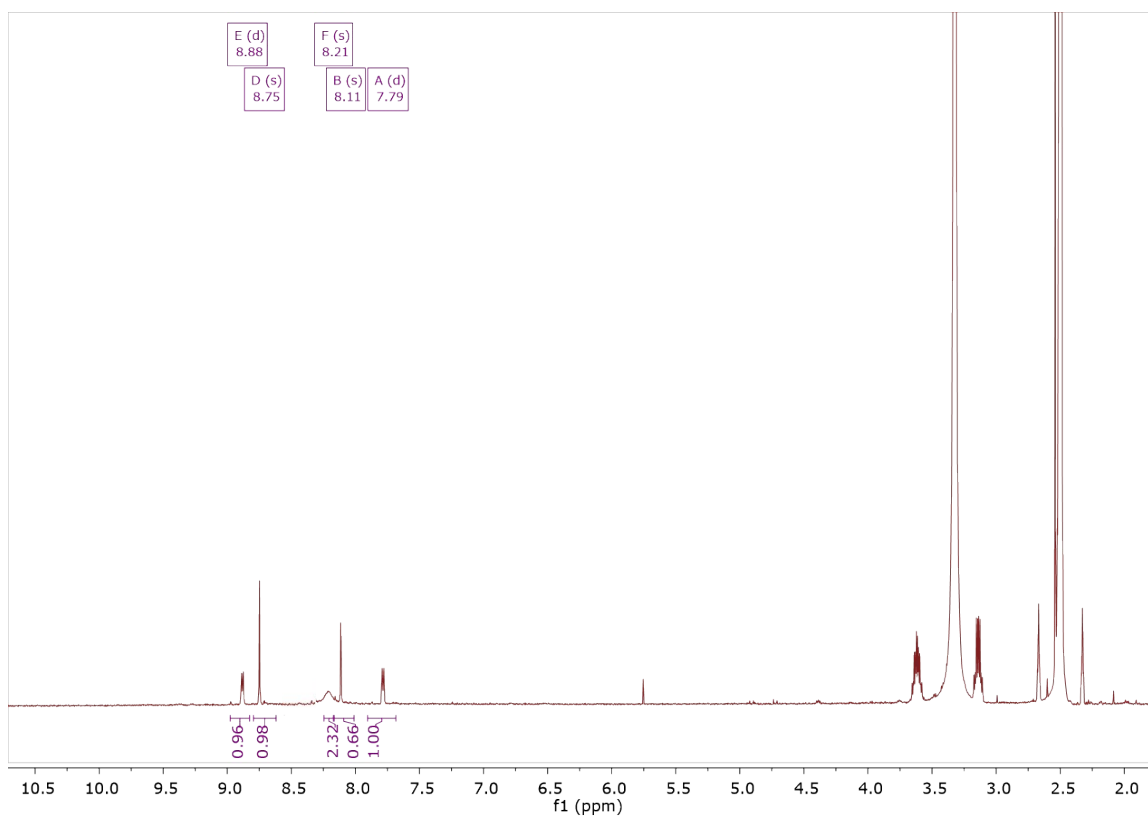


Figure S30. ¹H NMR spectrum of complex **4-CF₃** in DMSO-*d*⁶.

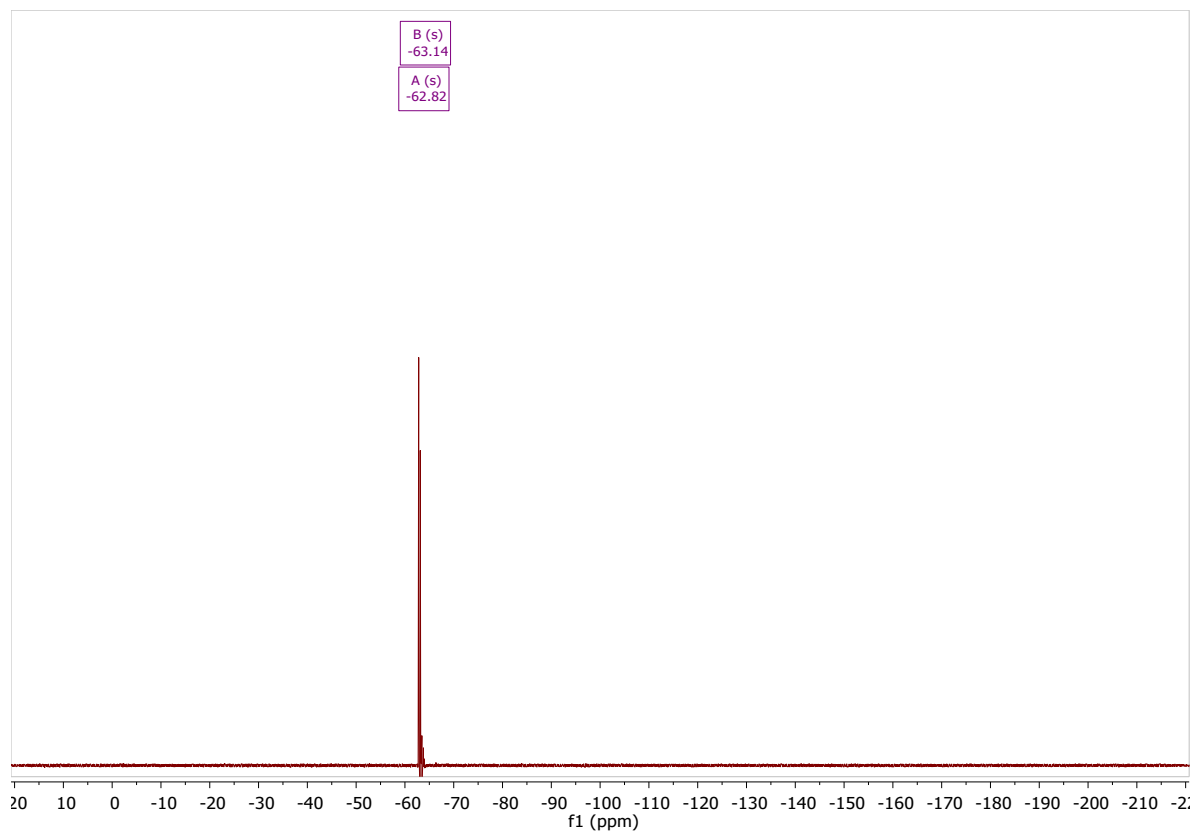


Figure S31. ^{19}F NMR spectrum of complex 4-CF_3 in $\text{DMSO-}d^6$.

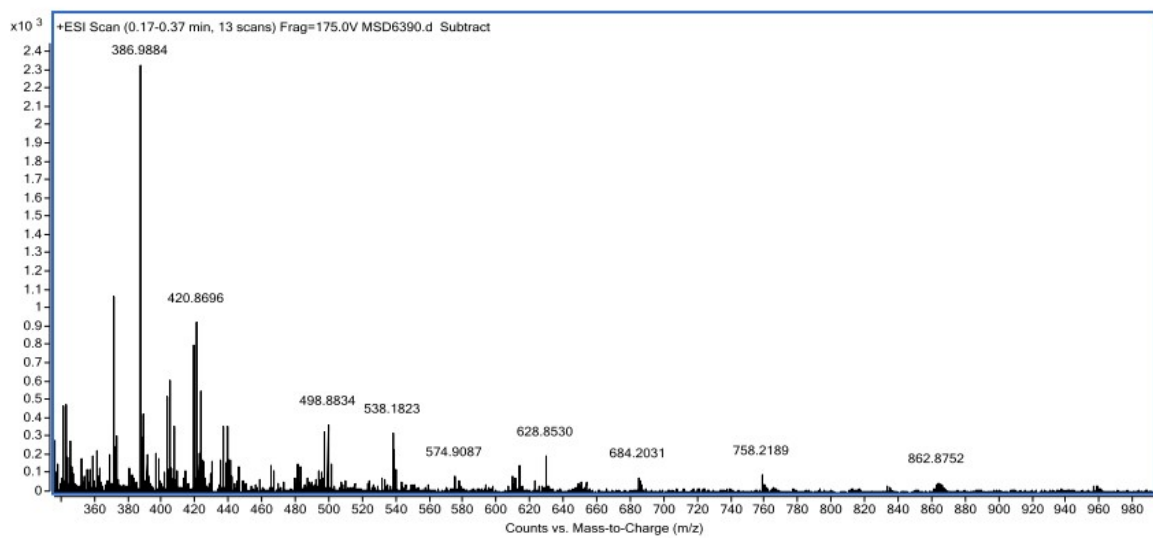


Figure S32. ESI-TOF(+) of complex 4-CF_3 .

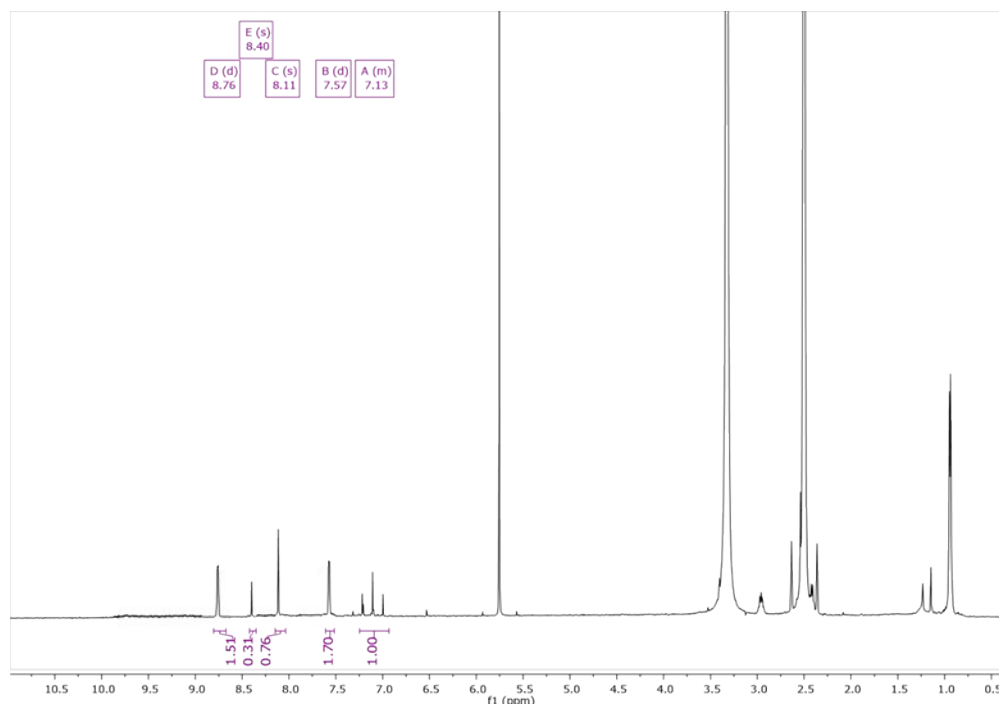


Figure S33. ^1H NMR spectrum of complex **4-CHF₂** in $\text{DMSO-}d^6$.

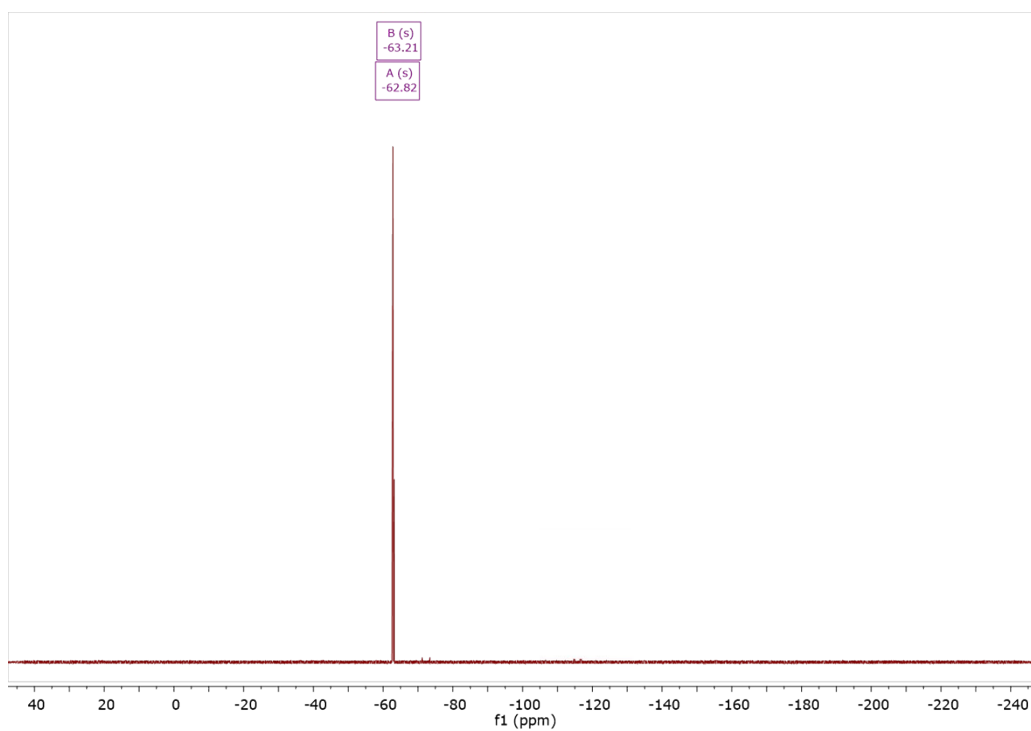


Figure S34. ^{19}F NMR spectrum of complex **4-CHF₂** in $\text{DMSO-}d^6$.

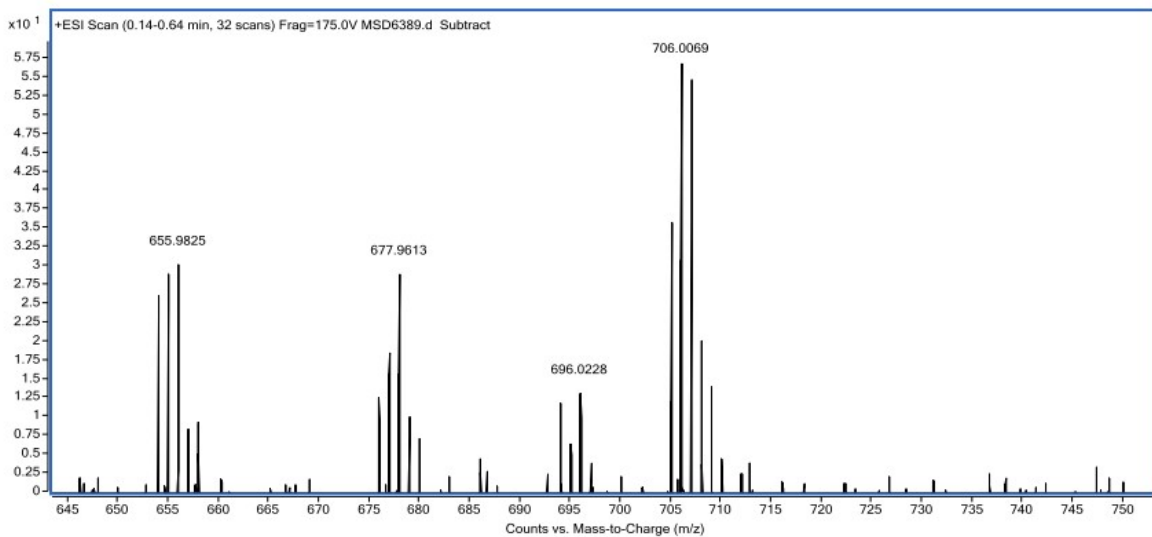


Figure S35. ESI-TOF(+) of complex **4-CHF₂**.

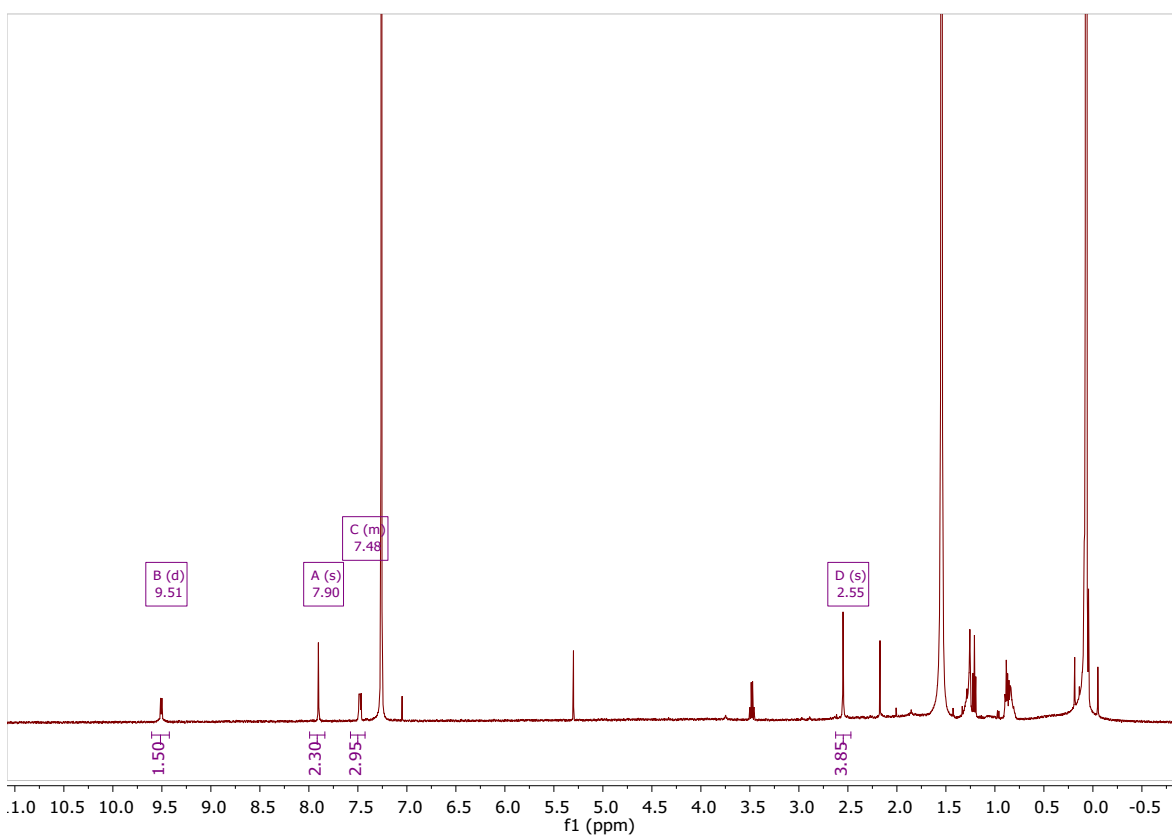


Figure S36. ¹H NMR spectrum of complex **4-CH₃** in CDCl₃.

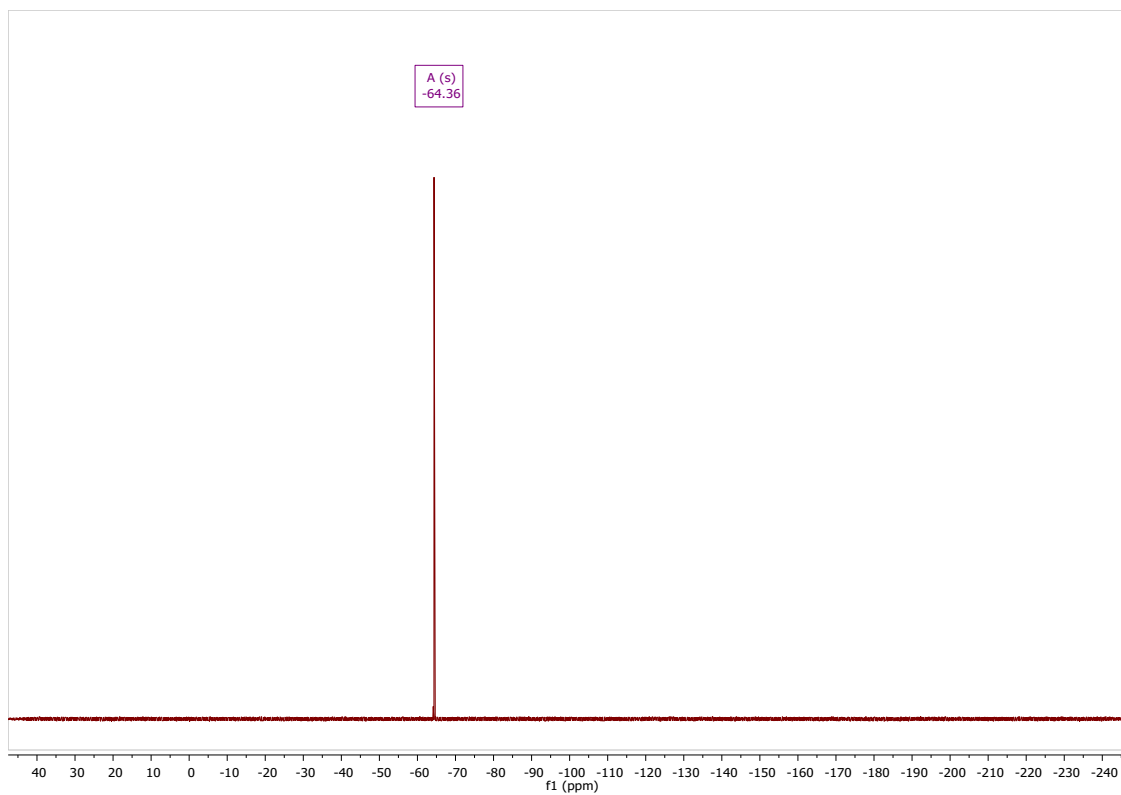


Figure S37. ^{19}F NMR spectrum of complex **4-CH₃** in CDCl_3 .

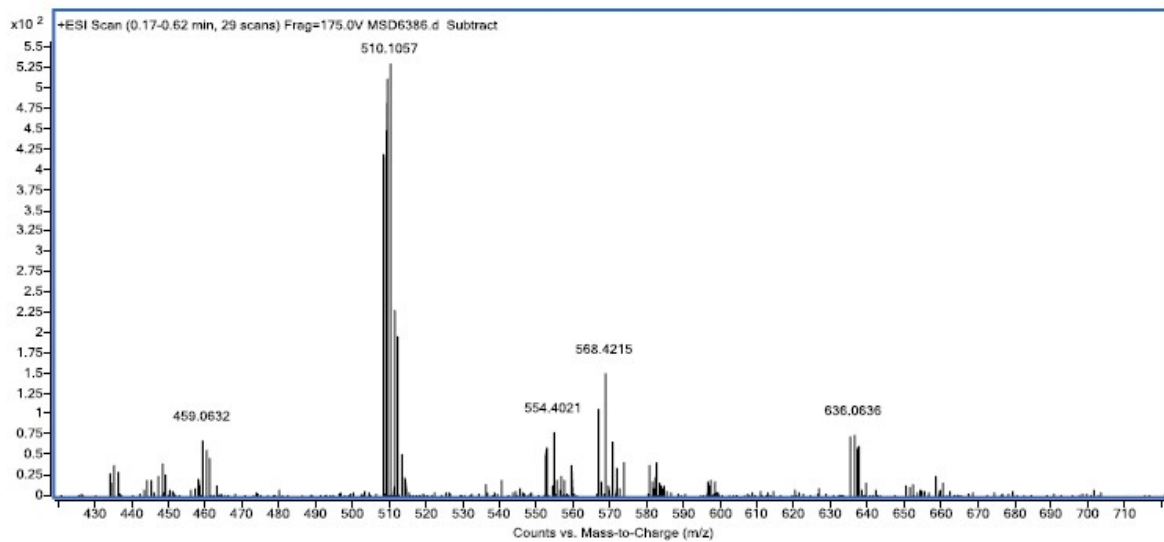


Figure S38. ESI-TOF(+) of complex **4-CH₃**.

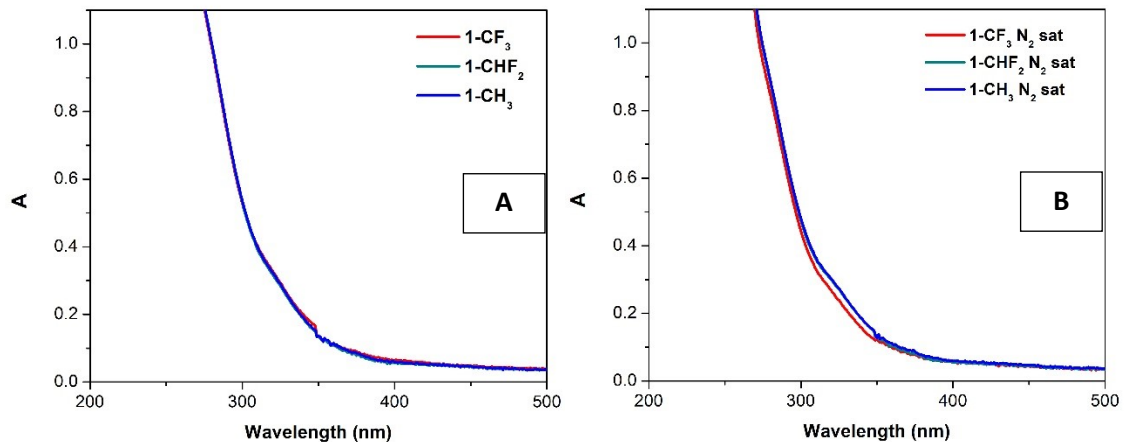


Figure S39. Absorption spectra of 10^{-5} M DMSO air-equilibrated (A) and N_2 saturated solutions of compounds **1-CF₃**, **1-CHF₂**, and **1-CH₃**.

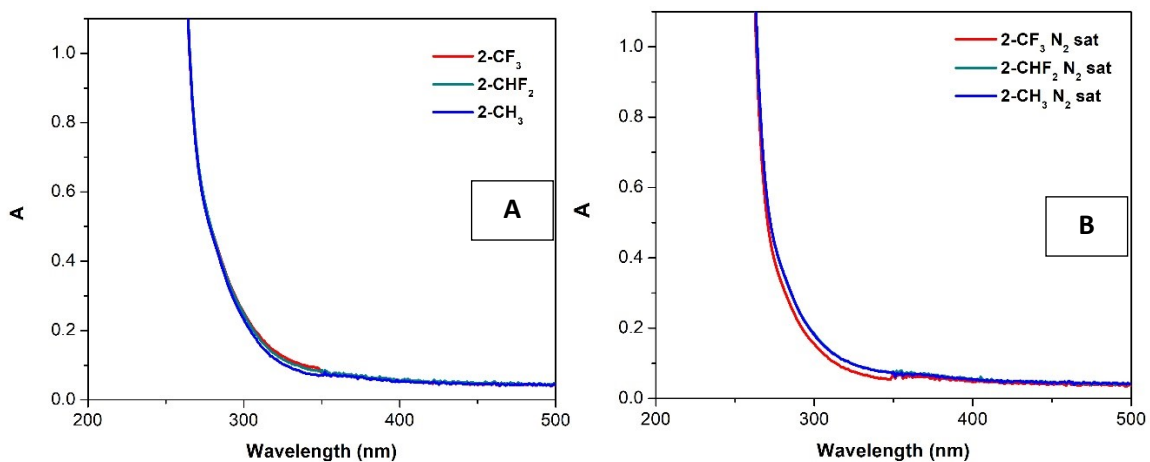


Figure S40. Absorption spectra of 10^{-5} M DMSO air-equilibrated (A) and N_2 saturated solutions of compounds **2-CF₃**, **2-CHF₂**, and **2-CH₃**.

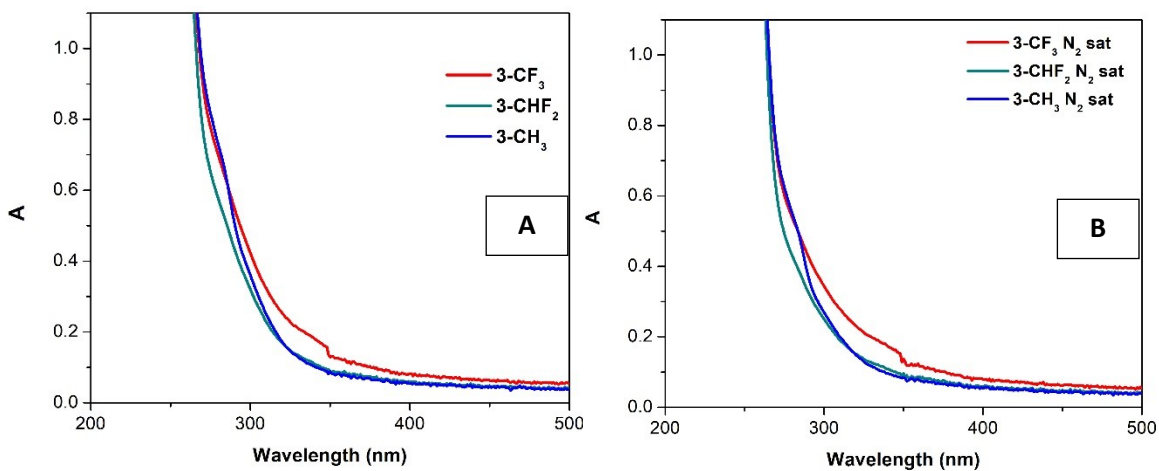


Figure S41. Absorption spectra of 10^{-5} M DMSO air-equilibrated (A) and N_2 saturated solutions of compounds **3-CF₃**, **3-CHF₂**, and **3-CH₃**.

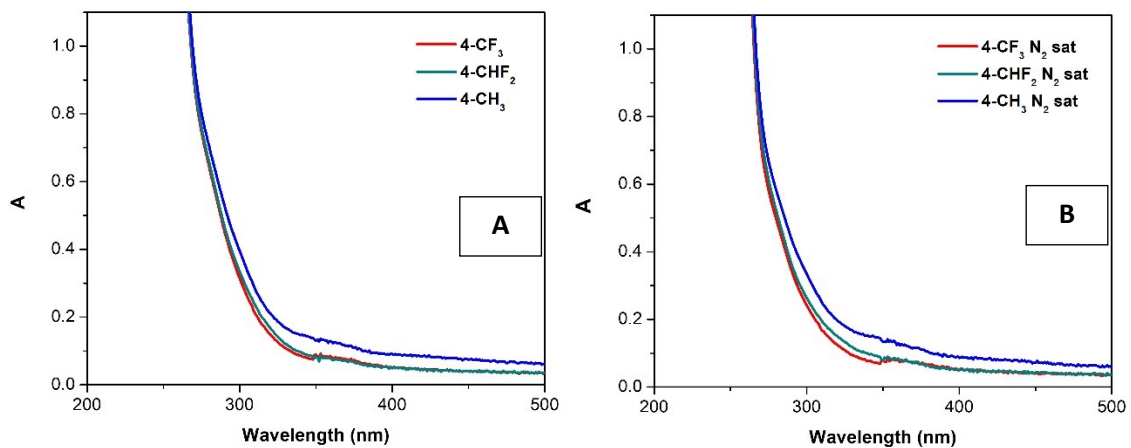


Figure S42. Absorption spectra of 10^{-5} M DMSO air-equilibrated (A) and N_2 saturated solutions of compounds **4-CF₃**, **4-CHF₂**, and **4-CH₃**.

Table S1. Calculated wavelengths of absorption, transition energies, and oscillator strength computed at the CAM-B3LYP/def2-TZVP level

Complex	Wavelength (nm)	Energy (eV)	Oscillator strength	Transitions
1-CF₃	376	3.298	0.0170	S ₀ →S ₁
	305	4.060	0.0160	S ₀ →S ₂
1-CHF₂	375	3.308	0.0184	S ₀ →S ₁
	305	4.062	0.0158	S ₀ →S ₂
1-CH₃	373	3.327	0.0204	S ₀ →S ₁
	304	4.084	0.0159	S ₀ →S ₂
2-CF₃	382	3.244	0.0184	S ₀ →S ₁
2-CHF₂	381	3.256	0.0201	S ₀ →S ₁
2-CH₃	379	3.271	0.0220	S ₀ →S ₁
3-CF₃	338	3.670	0.0098	S ₀ →S ₁
3-CHF₂	337	3.674	0.0100	S ₀ →S ₁
3-CH₃	337	3.682	0.0100	S ₀ →S ₁
4-CF₃	341	3.633	0.0079	S ₀ →S ₁
4-CHF₂	341	3.637	0.0080	S ₀ →S ₁
	316	3.930	0.0002	S ₀ →S ₂
4-CH₃	341	3.639	0.0079	S ₀ →S ₁
	314	3.941	0.0000	S ₀ →S ₂

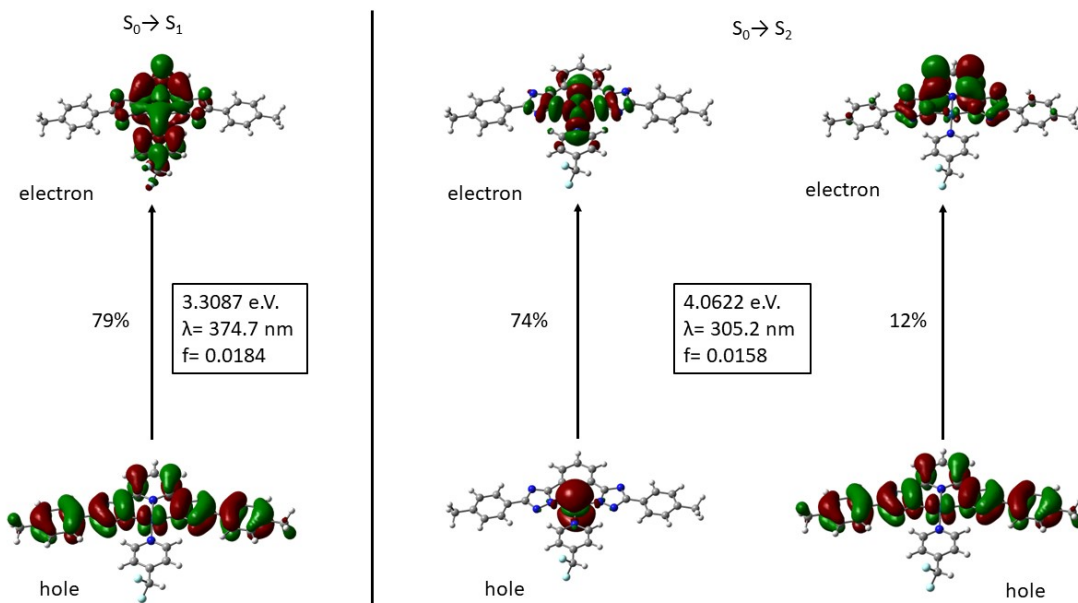


Figure S34. Representation of the NTOs involved in the $S_0 \rightarrow S_1$ (left) $S_0 \rightarrow S_2$ (right) excitation of compound **1-CHF₂**, with indication of the theoretical λ_{exc} , oscillator strength and relative contribution of each NTO pair.

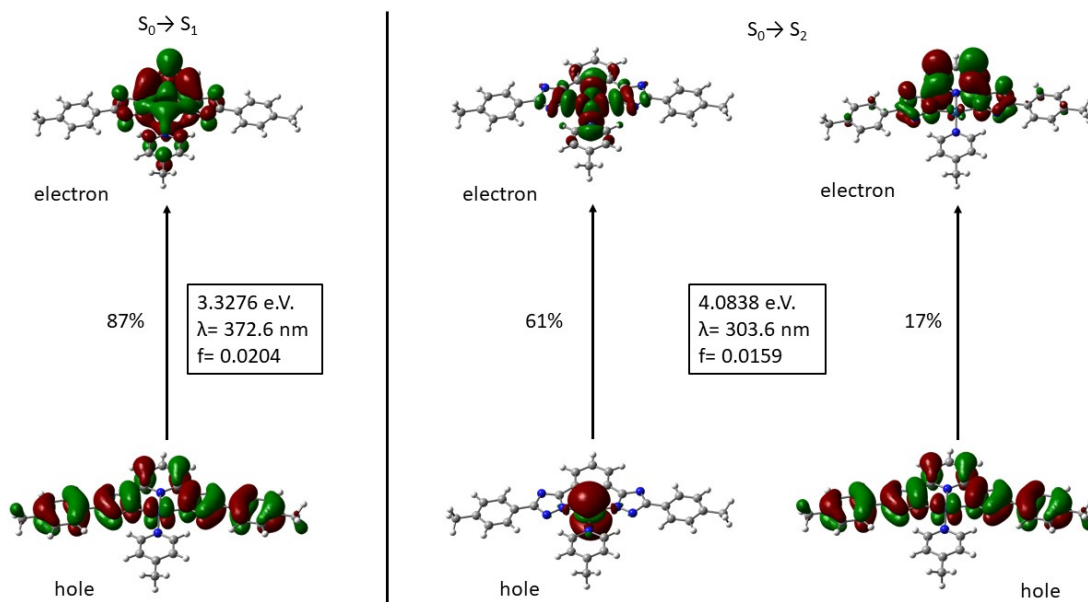


Figure S44. Representation of the NTOs involved in the $S_0 \rightarrow S_1$ (left) $S_0 \rightarrow S_2$ (right) excitation of compound **1-CH₃**, with indication of the theoretical λ_{exc} , oscillator strength and relative contribution of each NTO pair.

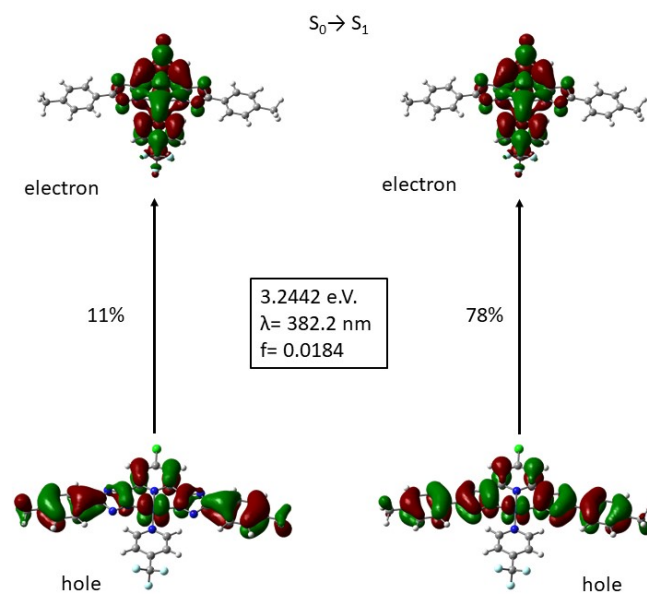


Figure S45. Representation of the NTOs involved in the $S_0 \rightarrow S_1$ excitation of compound **2-CF₃**, with indication of the theoretical λ_{exc} , oscillator strength and relative contribution of each NTO pair.

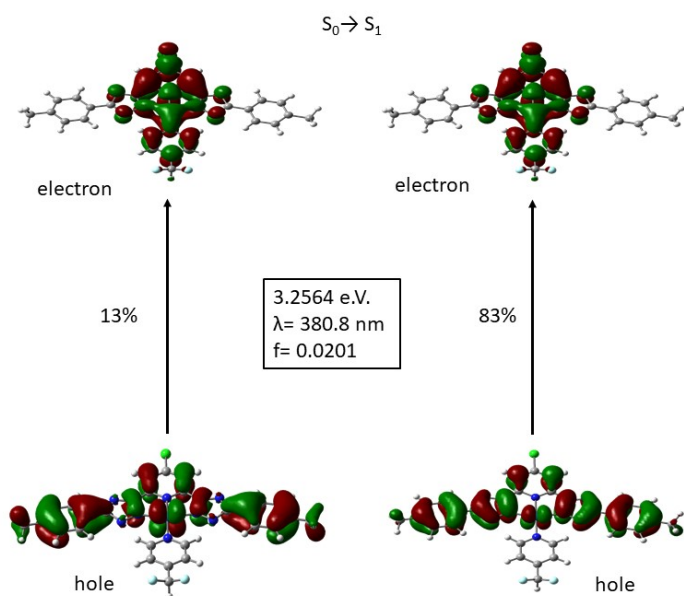


Figure S46. Representation of the NTOs involved in the $S_0 \rightarrow S_1$ excitation of compound **2-CHF₂**, with indication of the theoretical λ_{exc} , oscillator strength and relative contribution of each NTO pair.

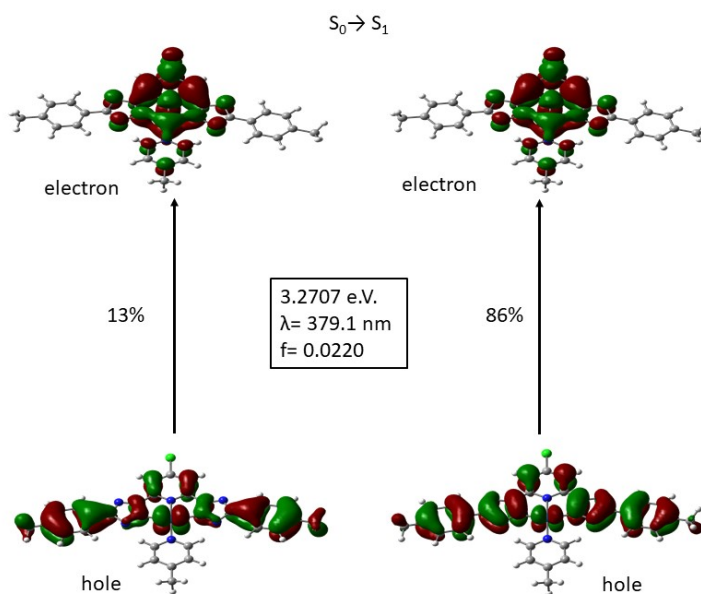


Figure S47. Representation of the NTOs involved in the $S_0 \rightarrow S_1$ (left) excitation of compound **2-CH₃**, with indication of the theoretical λ_{exc} , oscillator strength and relative contribution of each NTO pair.

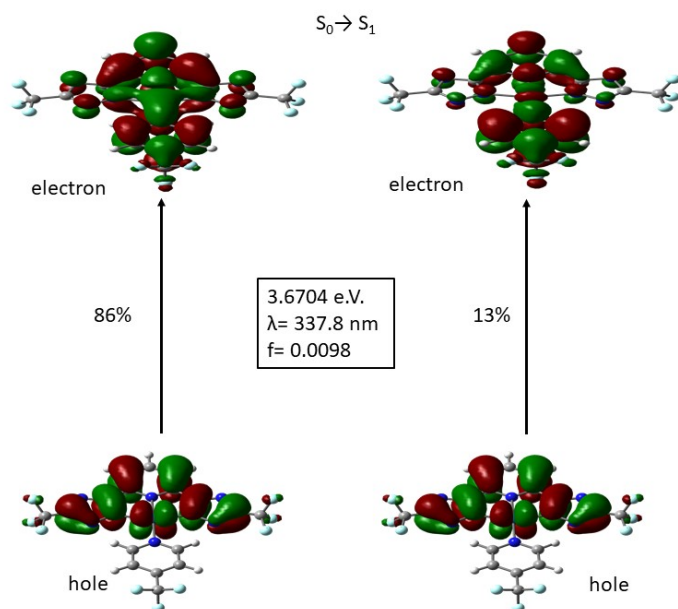


Figure S48. Representation of the NTOs involved in the $S_0 \rightarrow S_1$ excitation of compound **3-CF₃**, with indication of the theoretical λ_{exc} , oscillator strength and relative contribution of each NTO pair.

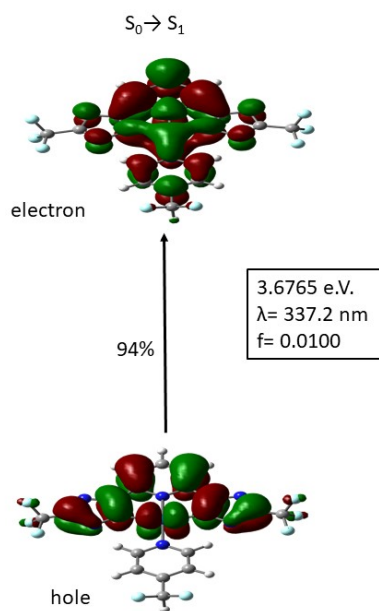


Figure S49. Representation of the NTOs involved in the $S_0 \rightarrow S_1$ excitation of compound **3-CHF₂**, with indication of the theoretical λ_{exc} , oscillator strength and relative contribution of each NTO pair.

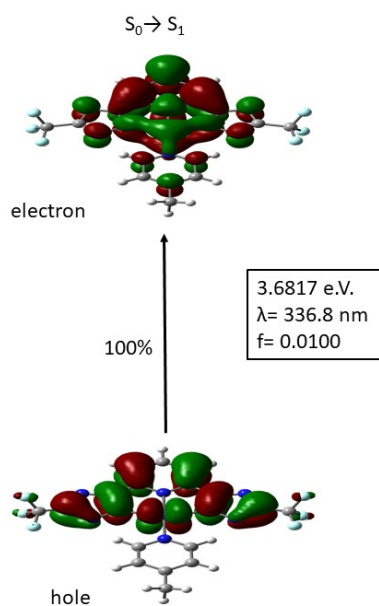


Figure S50. Representation of the NTOs involved in the $S_0 \rightarrow S_1$ excitation of compound **3-CH₃**, with indication of the theoretical λ_{exc} , oscillator strength and relative contribution of each NTO pair.

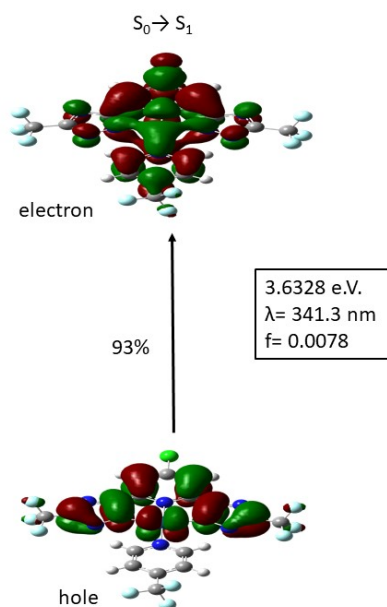


Figure S51. Representation of the NTOs involved in the $S_0 \rightarrow S_1$ excitation of compound **4-CF₃**, with indication of the theoretical λ_{exc} , oscillator strength and relative contribution of each NTO pair.

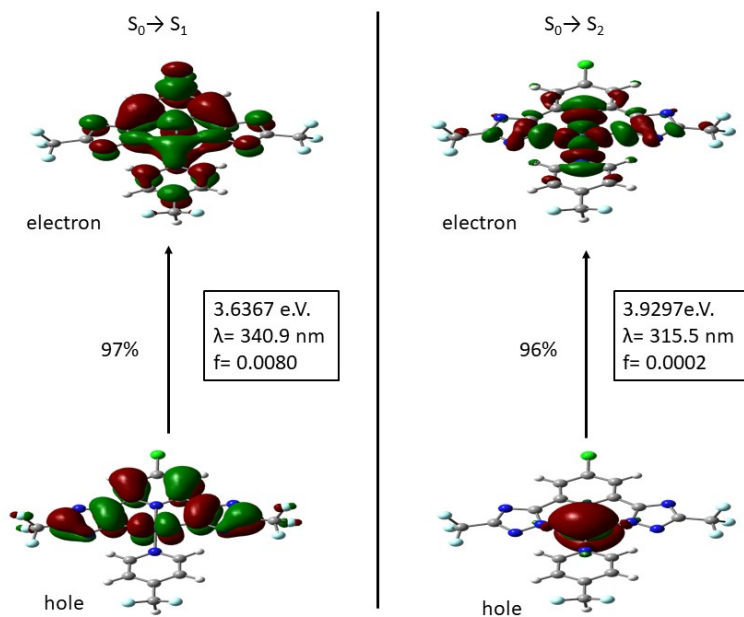


Figure S52. Representation of the NTOs involved in the $S_0 \rightarrow S_1$ (left) $S_0 \rightarrow S_2$ (right) excitation of compound **4-CHF₂**, with indication of the theoretical λ_{exc} , oscillator strength and relative contribution of each NTO pair.

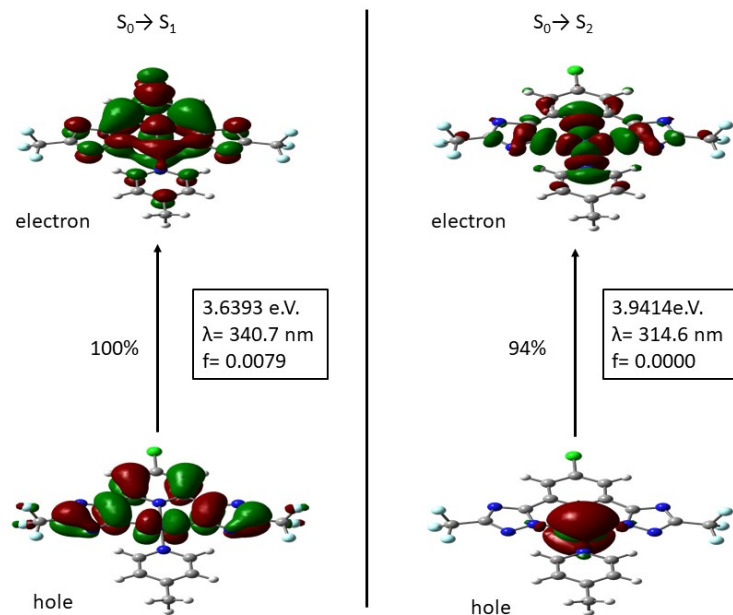


Figure S53. Representation of the NTOs involved in the $S_0 \rightarrow S_1$ (left) $S_0 \rightarrow S_2$ (right) excitation of compound **4-CH₃**, with indication of the theoretical λ_{exc} , oscillator strength and relative contribution of each NTO pair.

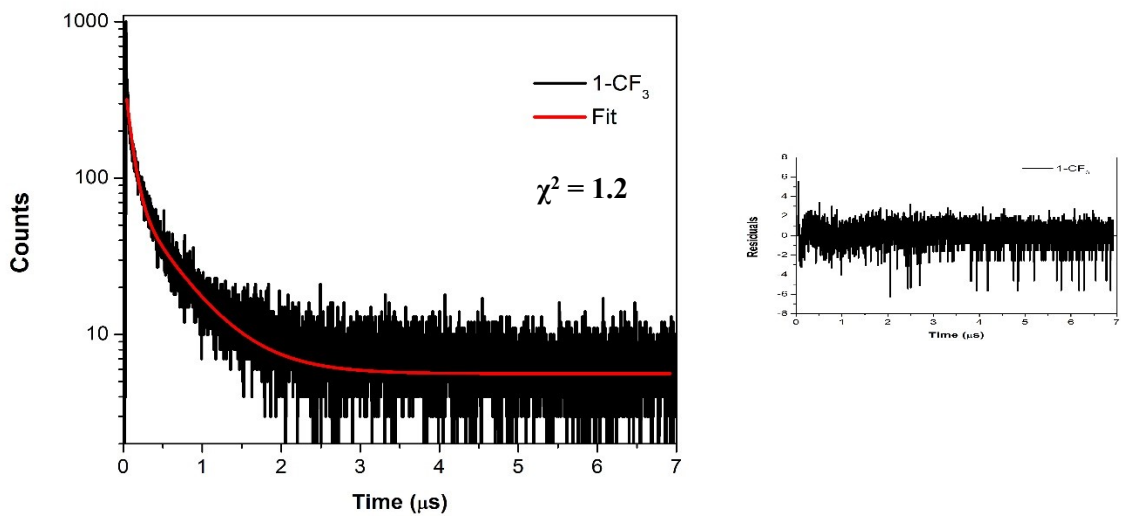


Figure S54. Phosphorescence lifetime and residuals of **1-CF₃** in solid state.

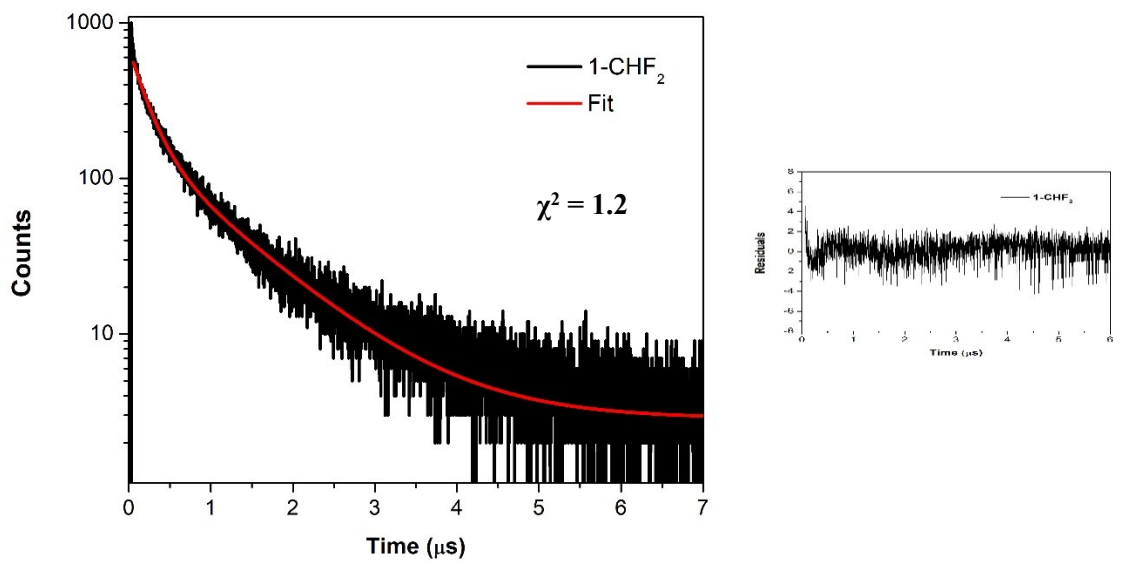


Figure S55. Phosphorescence lifetime and residuals of **1-CHF₂** in solid state.

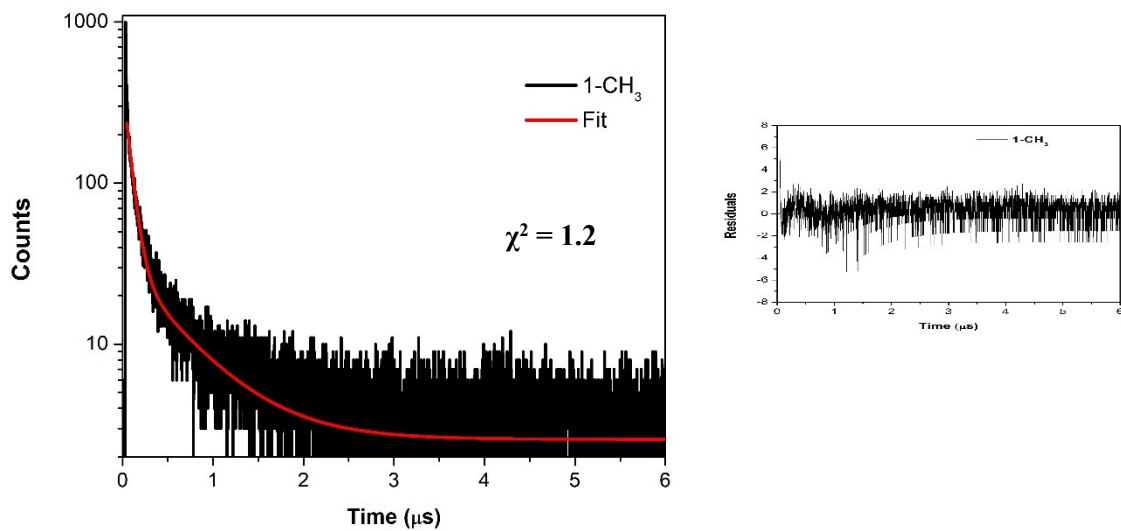


Figure S56. Phosphorescence lifetime and residuals of **1-CH₃** in solid state.

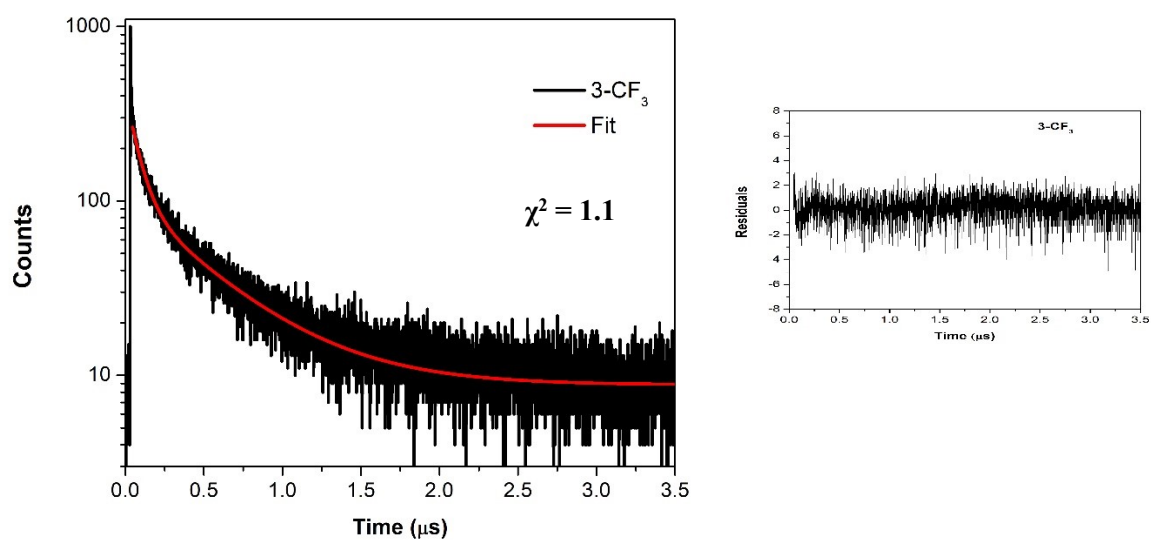


Figure S57. Phosphorescence lifetime and residuals of **3-CF₃** in solid state.

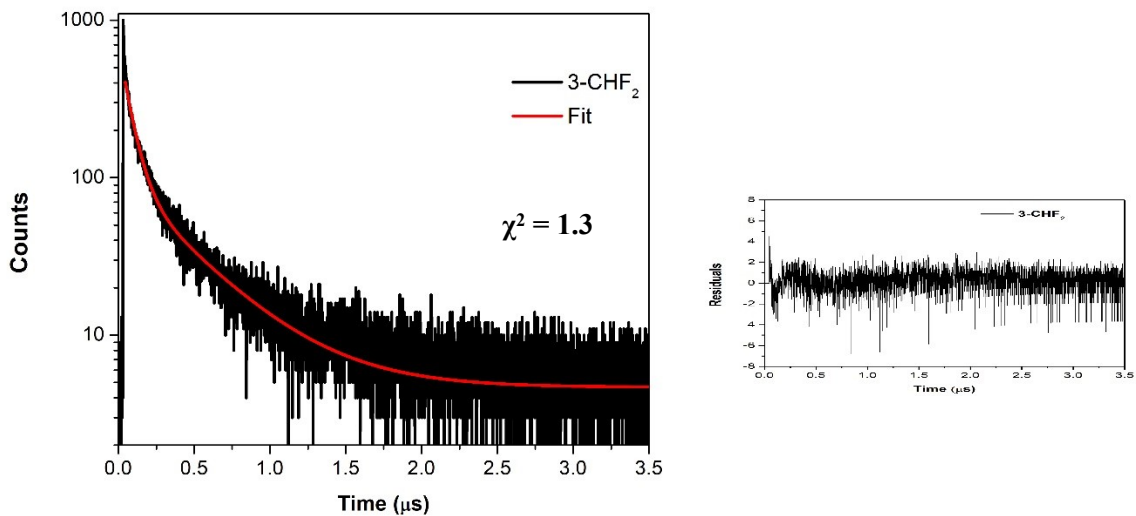


Figure S58. Phosphorescence lifetime and residuals of 3-CHF_2 in solid state.

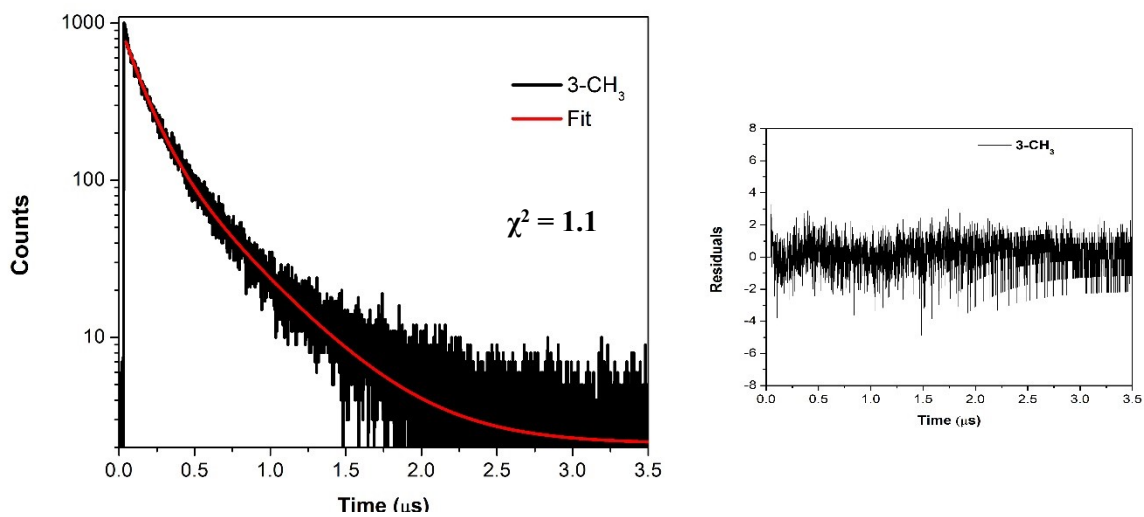


Figure S59. Phosphorescence lifetime and residuals of 3-CH_3 in solid state.

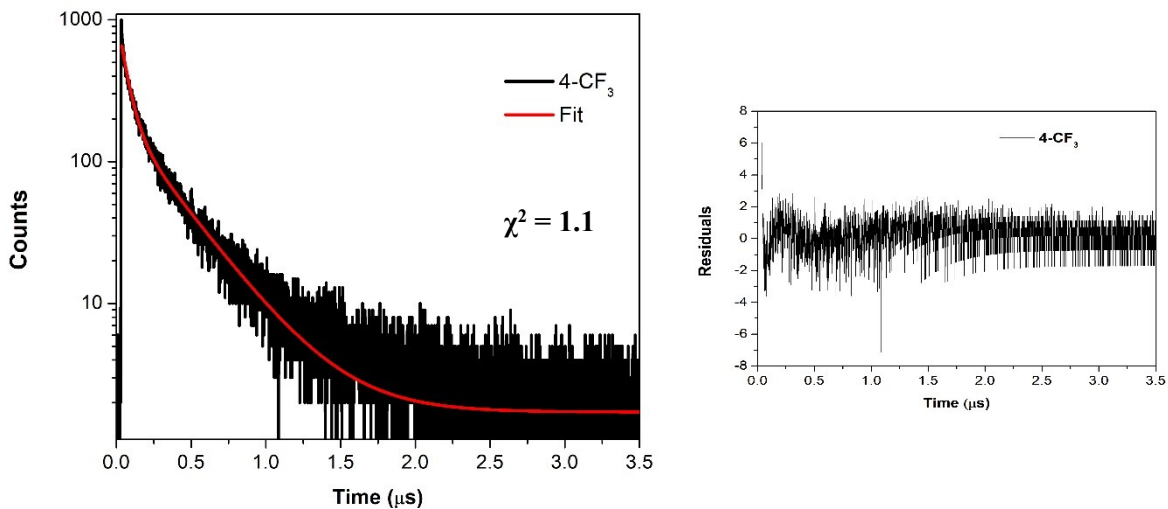


Figure S60. Phosphorescence lifetime and residuals of **4-CF₃** in solid state.

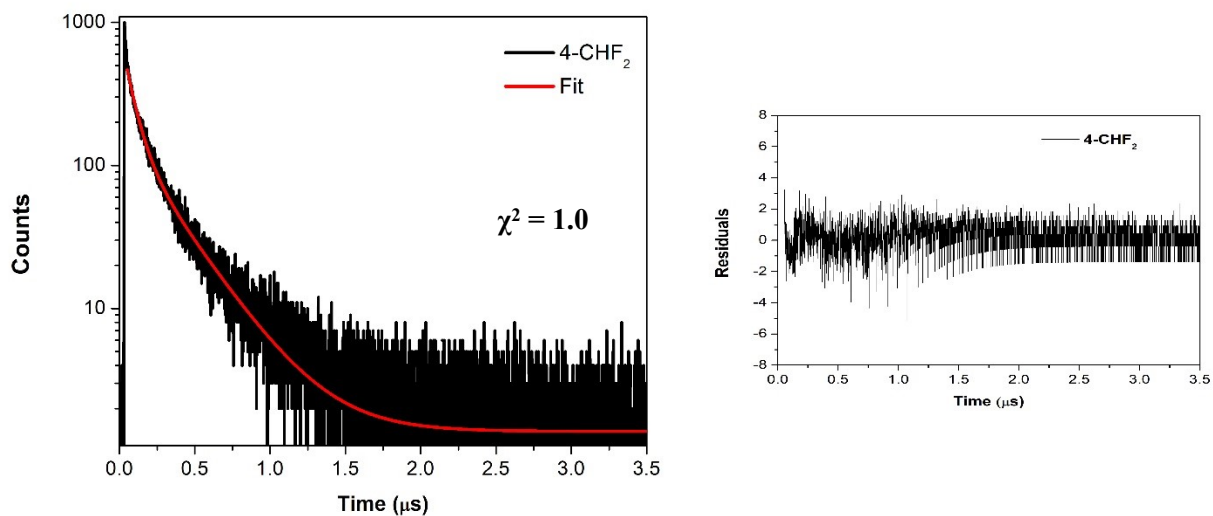


Figure S61. Phosphorescence lifetime and residuals of **4-CHF₂** in solid state.

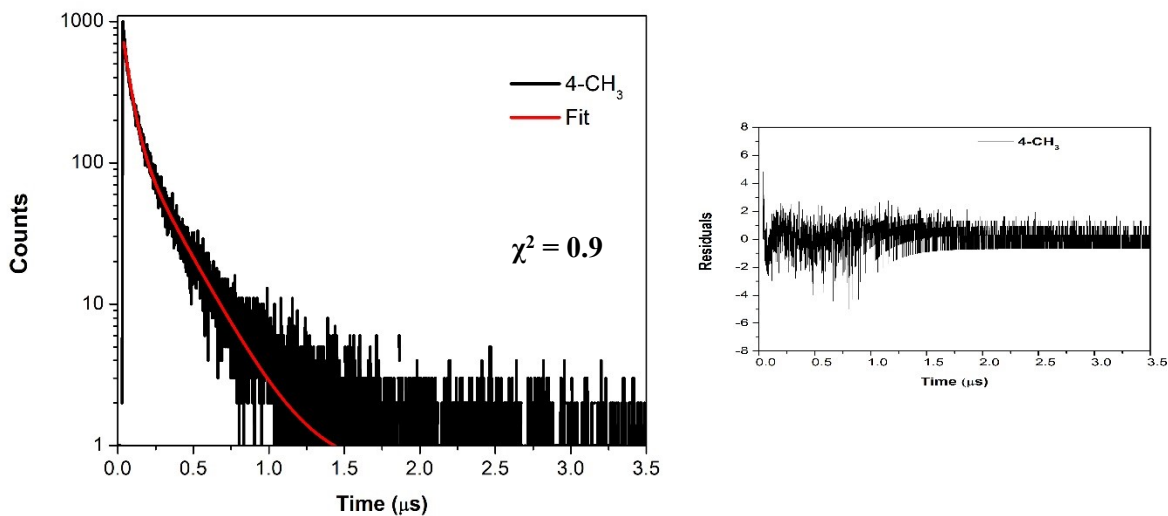


Figure S62. Phosphorescence lifetime and residuals of 4-CH₃ in solid state.

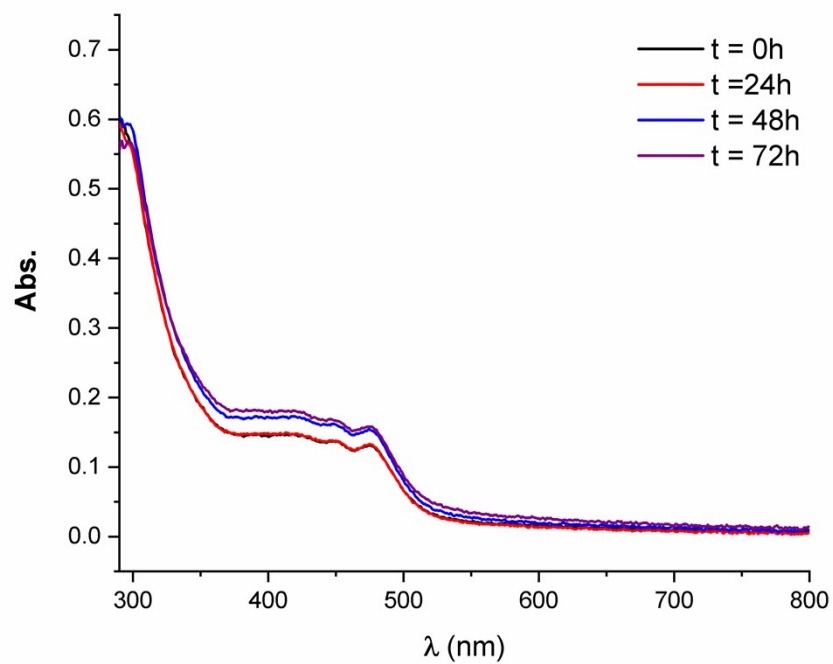


Figure S63. Stability of 1-CHF₂ in PBS and DMSO (5%) at 37 °C measured by UV-Vis.

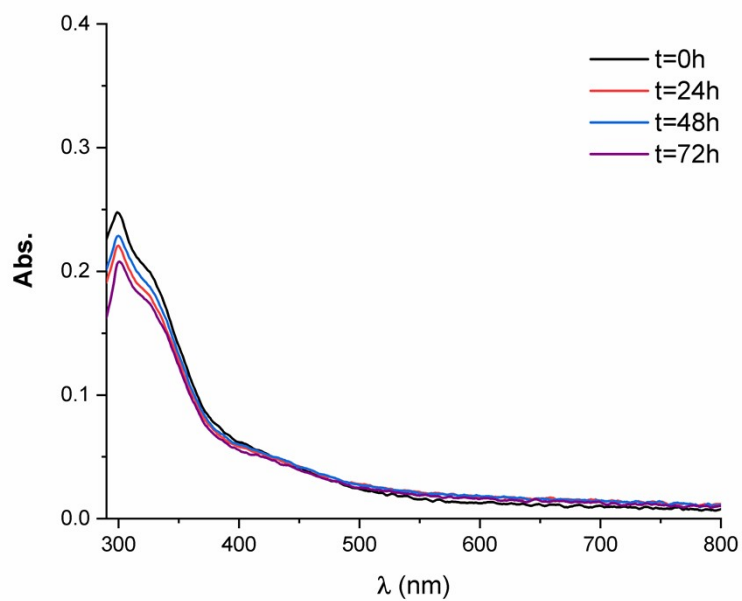


Figure S64. Stability of 1-CH₃ in PBS and DMSO (5%) at 37 °C measured by UV-Vis.

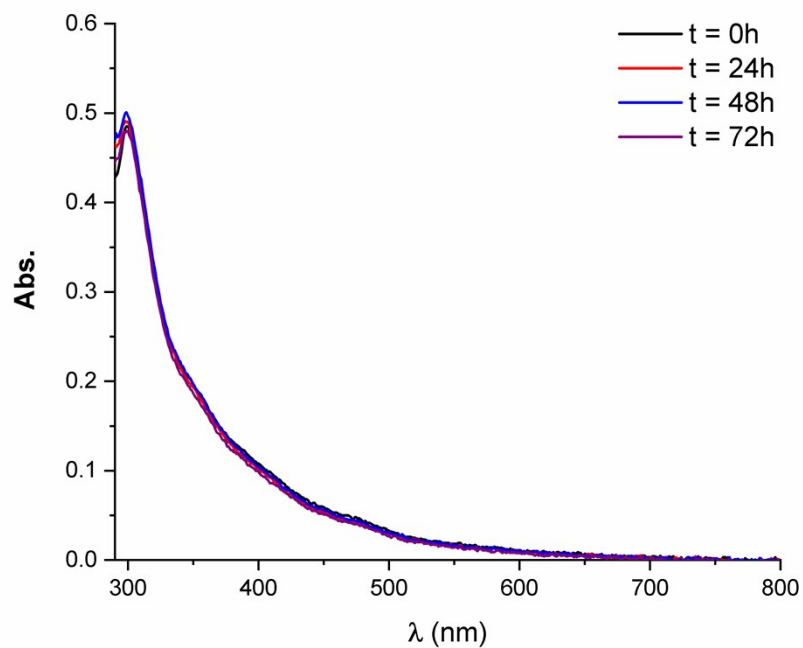


Figure S65. Stability of 2-CH₃ in PBS and DMSO (5%) at 37 °C measured by UV-Vis.



Figure S66. Stability of **3-CF₃** in PBS and DMSO (5%) at 37 °C measured by UV-Vis.

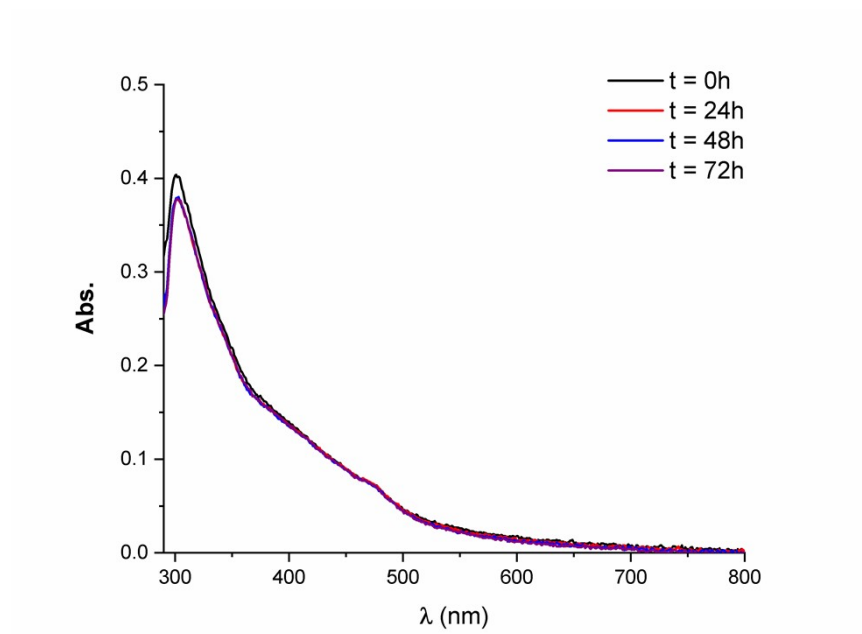


Figure S67. Stability of **3-CH₃** in PBS and DMSO (5%) at 37 °C measured by UV-Vis.

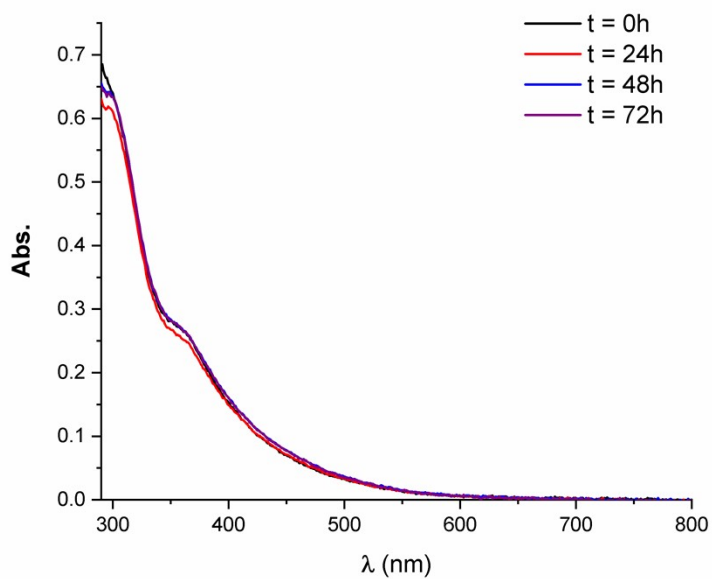


Figure S68. Stability of 4-CF₃ in PBS and DMSO (5%) at 37 °C measured by UV-Vis.

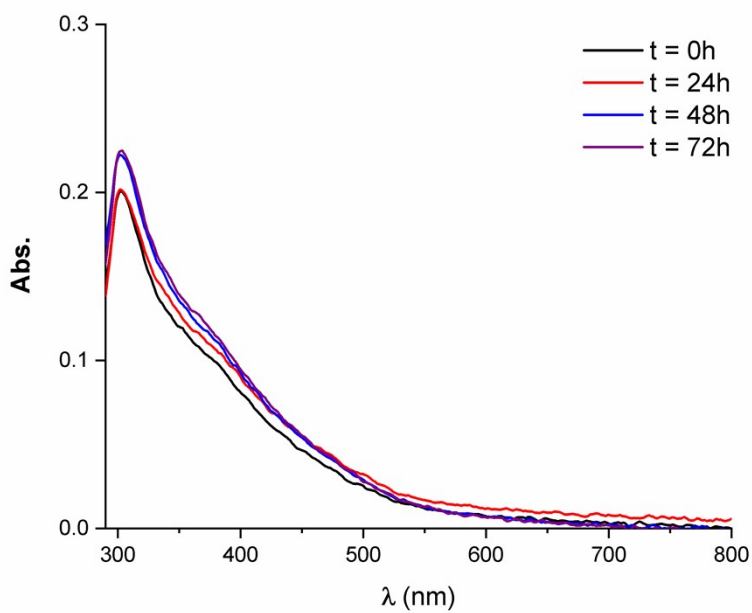


Figure S69. Stability of 4-CH₃ in PBS and DMSO (5%) at 37 °C measured by UV-Vis.